A Thesis

0n

STUDY ON BIOACTIVE AND STRUCTURAL PROPERTIES OF Na_2O MODIFIED GLASSESS

Submitted in the partial fulfillment of requirement for the award of the Degree of

Master of Technology

In

MATERIALS AND METALLURGICAL ENGINEERING

Submitted by

ISHVDEEP SINGH

Roll No- 600902004

Under the supervision of

Dr. Kulvir Singh

(Associate Professor)

SCHOOL OF PHYSICS AND MATERIAL SCIENCES

THAPAR UNIVERSITY

PATIALA-147001

JULY-2011

CERTIFICATE

I hereby certify that the entitled ***"Study on Bioactive and Structural Properties of Na_2O Modified Glasses"*** *submitted by* ***Mr. ISHVDEEP SINGH****, Roll No. 6009002004 in the partial fulfilment of the requirement for award of the degree of* ***MASTER OF TECHNOLOGY*** *in* ***"Materials and Metallurgical Engineering"*** *from the* ***School of Physics and Materials Science****, Thapar University Patiala. It is certify that the matter embodied in this report is of the candidate's own record not submitted to any other university in any part or full from for the award of such of a degree.*

Dr. Kulvir Singh
Associate Professor (Supervisor)
School of Physics and Material Science
Thapar University
Patiala-147001
India

Countersigned by:

Dr. O. P. Pandey
Professor and Head
SPMS
Thapar University
Patiala, Punjab
India

Dr. S. K. Mohapatra
Dean of Academic Affairs
Thapar University
Patiala, Punjab
India

ACKNOWLEDGEMENTS

At this momentous occasion of binding my thesis I would like to acknowledge the contribution of all those benevolent people, I have been blessed to associate with. Behind every student, there stand a myriad of people whose help and contribution makes things successful. Since such a list can be a prohibitively long, I may be excused for any omissions. My first and foremost offering of thanks goes to my supervisor **Dr. Kulvir Singh** (Associate Prof.) for providing me a chance to work under his guidance and supervision, assisting with all kinds of support and inspiration, wide counsel, constant encouragement, sincere criticism, valuable suggestions, expertise and fruitful advice which they proffered throughout this investigation and preparation of the thesis.

My greatest thanks are to **Dr. O.P.Pandey**, Prof. and Head, School of Physics and Material Science, Thapar University, Patiala. He has been very helpful in improving. I am grateful to him for sharing his time and expertise. My special thanks all the faculties and staff of School of Physics and Materials Science are acknowledged who never turn me down whenever I approached for any help .My special thanks to P.G Lab incharge **Mr. Purushottam** and **Mr. Jant Singh** for providing all kind of help for creating a healthy environment.

Words are inadequate in expressing my sincere thanks to Research Scholars **Mrs. Bhupinder kaur** for her support in every moment of difficulty. Her skills, fruitful discussion, constructive suggestions and constant inspiration in this work helped me to fulfill this effort.

I would also like to give my thanks to my friends **Mr. Khushwinder Singh Samra, Mr Gurpreet Singh Sandhu, Ms. Chandani Khurana, Mr. Paramjyot Jha, Mr. Praveen Jha, Mr. Mukul Verma, Ms. Andeep Kaur Shoker, Ms. Gagndeep Kaur Rosha, Ms. Samita Thakur and Mr. Harjinder Singh** for their kind help and

valuable suggestions whenever I needed and for providing me a friendly atmosphere and encouraging me throughout this research.

Last but not least my father **Mr. Swarn Singh Shoker** and my mother **Mrs. Balwinder Kaur Shoker** are the two guiding pillars of my success. Especially my father whose constant motivation and financial assistance during thick and thin has been the sole source of inspiration and strength to carry on my work.

Above all, hidden force by **Almighty God** steered me in the right direction to achieve the goal.

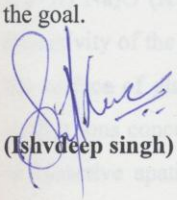

(Ishvdeep singh)

iii

ABSTRACT

Biomaterials are being used in medical devices or in contact with biological systems. They may be distinguished from other materials in that they possess a combination of properties, including chemical, mechanical, physical and biological properties that render them suitable for safe, effective and reliable use within a physiological environment.

In this study glasses with composition (55-X) SiO_2 -10 Al_2O_3 -15 CaO -5 TiO_2 – (10+X) Na_2O (X = 5, 10, 15 mol %) were prepared by melt-quenching technique. Bioactivity of the glasses was investigated in vitro by examining apatite formation on the surface of glasses after dipping in a simulated body fluid (SBF), SBF solution exhibit ions concentrations nearly equal to those in human blood plasma. Formation of bioactive apatite layer on the samples treated in SBF was confirmed by using Fourier transform infrared reflection (FTIR) spectroscopy, X-ray diffraction (XRD) and scanning electron microscope (SEM) equipped with energy dispersive X-ray spectrometer. Development of an apatite structure on the surface of the SBF treated glass samples as functions of composition and time could be established using the XRD data.

FTIR spectra of the glasses treated in SBF show some fundamental changes which is related to formation of apatite after 14-day of immersion in SBF. SEM observations revealed that the spherical particles formed on the glass surface were made of calcium and phosphorus. Increase in bioactivity with increasing sodium oxide content was observed. The results have been used to understand the evolution of the apatite surface layer as a function of glass composition and immersion time in SBF. The XRD pattern and band gap measurement clearly indicate some modification on the surface of the glasses which is manifestation of the apatite formation

CONTENTS

LIST OF FIGURES

LIST OF TABLES

CHAPTER-1

INTRODUCTION

In the past, there was no targeted based scientific development of biomaterials. Instead, devices consisting of materials that had been designed, synthesized and fabricated for various industrial needs (for example the textile, aerospace, and defence industries) were tested in a trial-and-error fashion on bodies of animals and humans. These unplanned and sporadic attempts had modest success. Most frequently, the results were unpredictable, mixed and confounding both in success and in failure.

Because of the continuous and ever-expanding practical needs of medicine and health care practice, there are currently thousands of medical devices, diagnostic products, and disposables on the market. Estimated annual sales of such products in the United States alone are in the order of one hundred billion dollars. In fact, the range of applications continues to grow. In addition to traditional medical devices, diagnostic products, pharmaceutical preparations and health care disposables, now the list of biomaterial applications includes smart delivery systems for drugs, tissue cultures, engineered tissues, and hybrid organs. To date, tens of millions of people have received medical implants.

Undoubtedly, biomaterials have had a major impact on the practice of contemporary medicine and patient care in both saving and improving the quality of lives of humans and animals. Modern biomaterial practice still takes advantage of developments in the traditional, nonmedical materials field but is also the biocompatibility and bio-functionality of implants.

1.1 BIOMATERIALS

Biomaterials is a term used to indicate materials that constitute parts of medical implants, extracorporeal device and disposables that have been utilized in medicine, surgery, dentistry and veterinary medicine as well as in every aspect of patient health care. The National Institutes of Health Consensus Development Conference defined a biomaterial

as ‘‘any substance (other than a drug) or combination of substances, synthetic or natural in origin, which can be used for any period of time, as a whole or as a part of a system which treats, augments, or replaces any tissue, organ, or function of the body’’ (Boretos and Eden, 1984). The common denominator in all the definitions that have been proposed for ‘‘biomaterials’’ is the undisputed recognition that biomaterials are distinct from other classes of materials because of the special biocompatibility criteria they must meet.

Admittedly, any current definition of biomaterials is neither perfect nor complete but has provided an excellent reference or starting point for discussion. It was inevitable that such a definition would need updating to reflect both the evolution and revolution in the dynamic biomedical field. For example, there is an increased emphasis on developing non-traditional clinical methodologies such as preventing and curing major genetic diseases. These trends in medicine present unique challenges for the biomaterials field. Applications such as controlled delivery of pharmaceuticals (drugs and vaccines), virally and non-virally mediated delivery agents for gene therapy and engineered functional tissues require vision, non-traditional thinking and novel design approaches. Most importantly, to meet the present and future biomaterials challenges successfully, we need materials scientists and engineers who are familiar with and sensitive to cellular, biochemical, molecular and genetic issues and who work electively in teams of professionals who include molecular biologists, biochemists, geneticists, physicians and surgeons.

Synthetic materials currently used for biomedical applications include metals and alloys, polymers and ceramics. These exhibits properties due to different structure.

1.2 CLASSIFICATION OF BIOMATERIALS

1.2.1 METALLIC BIOMATERIALS

Metals have been used almost exclusively for load-bearing implants such as hip and knee prostheses and fracture fixation wires, pins, screws and plates. Metals have also been used as parts of artificial heart valves, as vascular stents and as pacemaker leads. Although pure metals are sometimes used, alloys frequently provide improvement in materials properties such as strength and corrosion resistance. Three material groups

dominate biomedical metals: 316L stainless steel, cobalt-chromium-molybdenum alloy and pure titanium and titanium alloys (Table 1.1). The main considerations in selecting metals and alloys for biomedical applications are biocompatibility, appropriate mechanical properties, corrosion resistance and reasonable cost.

Table 1.1: Alloy implants and their compositions (wt. %).

Element	316L Stainless Steel (ASTMF138,139)	Co-Cr-Mo (ASTMF799)	Grade 4 Ti (ASTMF67)	Ti-6Al-4V (ASTMF136)
Al				5.5-6.5
C	.03 max	.035 max	0.010 max	0.08 max
Co		Balance		
Cr	17.0	26.0-30.0		
Fe	Balance	0.75 max	0.030-0.50	0.25 max
H			0.125-.015	0.0125 max
Mo	2.00	5.0-7.0		
Mn	2.00 max	1.0 max		
N		0.25 max	0.03-0.05	0.05 max
Ni	10.00	1.0 max		
O			0.18-0.40	0.13 max
P	0.03 max			
S	0.03 max			
Si	0.075 max	1.0 max		
Ti			Balance	Balance
V				3.5-4.5

1.2.1.1 Basic Properties of Metallic Biomaterials

The properties of materials are governed by their structure. At the atomic level, metals consist of positively charged ion cores immersed in a ‘‘cloud’’ of loosely bound electrons. This atomic level structure is responsible for the characteristic and distinct properties of metals. Metallic bonding allows the atoms to organize themselves into an ordered three-dimensional crystalline pattern, which can be visualized as the packing of hard spheres into cubic or hexagonal arrangements. The delocalized electrons are responsible for the electrical and thermal conductivity of metals. Because the interatomic bonds are not spatially directed in metals, planes of atoms can ‘‘slip’’ over one another to allow plastic deformation.

The chemical properties of materials also are related to the nature of their atomic bonding. The more resistant the constituent atoms/ions are to being separated, the more inert the material will be. In metals, non-directional way in which the electrons are bonded allows the atoms/ions to be parted more easily. Consequently, although their mechanical properties make metals the appropriate choice for many biomedical applications, susceptibility to chemical degradation is an aspect that must be considered.

Because the interactions between cells and tissues with biomaterials at the tissue implant interface are almost exclusively surface phenomena, surface properties of implant materials are of great importance. A surface is the termination of the normal three-dimensional structure of a material. Lack of near neighbour atoms on one side of the surface alters the electronic structure and consequently the way these atoms interact with other atoms. Chemical bonds will ‘‘dangle’’ into the space outside the solid material and will result in the surface atoms having higher energy than do atoms in the bulk. As a result, surface atoms will attempt to reduce free energy by rearranging or bonding to any available reactive molecules to reach a more favourable energy state.

1.2.1.2 Corrosion

The physiological environment is typically modelled as a 37 °C aqueous solution, at pH 7.3, with dissolved gases (such as oxygen), electrolytes, cells and proteins. Immersion of metals in this environment can lead to corrosion, which is deterioration and removal of

the metal by chemical reactions. During the electrochemical process of corrosion, metallic biomaterials can release ions, which may reduce the biocompatibility of materials and jeopardize the fate of implants. For example, the type and concentration of released corrosion products can alter the functions of cells in the vicinity of implants as well as of cells at remote locations after transport of the corrosion by-products to distant sites inside the body. These circumstances become stronger possibilities in the bodies of sick and elderly patients, who are the largest group of recipients of prostheses. Even before implantation, through chemical reaction of metals with the oxygen in ambient air or by oxidation in an acidic solution, an oxide surface film forms on their surface. Because oxides are ceramics, which are electrical and thermal insulators, the electrochemical reactions that lead to corrosion are reduced or prevented. In other words, the oxidized metallic surfaces are ‘‘passivated.’’ In fact, the stability of the oxides present on different metals determines their overall corrosion resistance. For example, even though 316L stainless steel implants perform satisfactorily in short-term applications, such as fracture fixation, they are susceptible to crevice corrosion and pitting when implanted for longer periods. Titanium and its alloys, as well as cobalt-chromium alloys, have more favourable corrosion resistance for long-term implant applications such as joint and dental prostheses.

1.2.1.3 Mechanical Properties

The mechanical properties of materials are of great importance when designing load-bearing orthopaedic and dental implants [1]. Some mechanical properties of metallic biomaterials are listed in Table 1.2. With a few exceptions, the high tensile and fatigue strength of metals, compared with ceramics and polymers, make them the materials of choice for implants that carry mechanical loads. It should be noted that, in contrast to the nano phase, composite nature of tissue such as bone, the biomedical metals used for implants are conventional, homogeneous materials. The elastic moduli of the metals listed in Table 1.2 are at least seven times greater than that of natural bone.

Table 1.2: Select Properties of Metallic Biomaterials.

Materials	Young's Modulus (GPa)	Yield Strength (MPa)	Tensile Strength (MPa)	Fatigue Limit (MPa)
Stainless steel	190	221-1,213	586-1,351	241-820
Cobalt-chromium (Co-Cr) alloys	210-253	448-1,606	655-1,896	207-950
Titanium (Ti)	110	485	760	300
Ti-6Al-4V	116	896-1,034	965-103	620
Cortical bone	15-30	30-70	70-150	

This mismatch of mechanical properties can cause ‘‘stress shielding,’’ a condition characterized by bone resorption (loss of bone) in the vicinity of implants. This clinical complication arises because preferential distribution of mechanical loading through the metallic prosthesis deprives bone of the mechanical stimulation needed to maintain homeostasis.

The mechanical properties of a specific implant depend not only on the type of metal but also on the processes used to fabricate the materials and device. Thermal and mechanical processing conditions can change the microstructure of materials. For example, in ‘‘cold-working’’ a metal such as by rolling or forging, the resulting deformation makes the materials stronger and harder. Unfortunately, as the metal becomes harder and stronger it also becomes less ductile and more chemically reactive.

Compared with the elastic moduli of either stainless steel or cobalt-chromium molybdenum alloys, Ti and Ti-6Al-4V have much lower (approximately half) moduli that are still almost an order of magnitude higher than that of bone. Another advantage of Ti-

based metals as a bone implant material is their favourable strength-to-density ratio. Stainless steel and Co-Cr alloys have densities of approximately 8.8 g/cm^3 and 7.8 g/cm^3 respectively. Because Ti has a density of only 4.5 g/cm^3, its strength-to-density ratio is larger. Disadvantages of titanium for medical use include relatively low shear strength, poor wear resistance and difficulties in fabrication. The stable, coherent titanium oxide (TiO_2) film that forms on titanium and its alloys gives them superior corrosion resistance compared with stainless steel and Co-Cr alloys. The oxidized surface is also believed to be responsible for Ti implants becoming Osseo integrated in vivo, a process whereby bone is opposed to the implant without chronic inflammation and without an intervening fibrous capsule.

1.2.2 CERAMIC AND GLASS BIOMATERIALS

Ceramics and glasses are used as components of hip implants, dental implants, middle ear implants and heart valves. Overall, these biomaterials have been used less extensively than either metals or polymers. Some ceramics that have been used for biomedical applications are listed in Table 1.3.

Table 1.3: Common ceramics and their use in Biomedical Applications.

Ceramic	Chemical Formula	Comment
Alumina	Al_2O_3	Bio inert
Zirconia	ZrO_2	Bio inert
Pyrolytic carbon	$Na_2OCaP_2O_3$-SiO_2	Bioactive
Hydroxyapatite (sintered at high temperature)	$Ca_{10}(PO_4)_6(OH)_2$	Bioactive
Hydroxyapatite (sintered at low temperature)	$Ca_{10}(PO_4)_6(OH)_2$	Biodegradable
Tricalcium phosphate	$Ca_{10}(PO4)(OH)_2$	Biodegradable

Definitions:

Bioinert refers to a material that retains its structure in the body after implantation and does not induce any immunologic host reactions.

Bioactive refers to materials that form bonds with living tissue.

Biodegradable refers to materials that degrade (by hydrolytic breakdown) in the body while they are being replaced by regenerating natural tissue; the chemical by-products of the degrading materials are absorbed and released via metabolic processes of the body.

1.2.2.1 Basic Properties of Ceramic Biomaterials

Ceramics are materials composed of metallic and non-metallic elements held together by ionic or covalent bonds. As with metals, the interatomic bonds in ceramics result in long-range three-dimensional crystalline structures; glasses do not have long-range order. In contrast to metallic bonding, the electrons in ionic and covalent bonds are localized between the constituent ions/atoms. Consequently, ceramics are typically electrical and thermal insulators. The strong ionic and covalent bonds also make ceramics hard and brittle, because the planes of atoms/ions cannot slip past one another. Ceramics and glasses typically fail with little plastic deformation and they are sensitive to the presence of cracks or other defects. The ionic or covalent nature of ceramics also influences their chemical behaviour.

1.2.2.2 Degradation/ Corrosion

Although they do not undergo corrosion, ceramics and glasses [2] are susceptible to other forms of degradation when exposed to the physiological environment. However, the mechanism and rate of degradation depend on the particular type of ceramic. Even alumina, which is generally considered a bio inert ceramic, experiences a time-dependent decrease in strength during immersion in saline in vitro and after implantation. This process may result from a preferential dissolution of impurities that result in crack propagation. Bioactive ceramics and glasses are also degraded in the body. Not only can they undergo slow or rapid dissolution (depending on the composition and processing

history of the material), but because of the similarity of calcium phosphates to the mineral component of bone, they may also be resorbed by osteoclasts (the cells that break down bone).

1.2.2.3 Mechanical Properties

The major drawbacks to the use of ceramics and glasses as implants are their brittleness and poor tensile properties (Table 1.4). Although they can have outstanding strength when loaded in compression, ceramics and glasses fail at low stress when loaded in tension or bending. Among biomedical ceramics, alumina has the highest mechanical properties, but its tensile properties are still below those of metallic biomaterials [3-4]. Additional advantageous properties of alumina are its low coefficient of friction and wear rate. Because of these properties, alumina has been used as a bearing surface in joint replacements. The mechanical properties of calcium phosphates and bioactive glasses make them unsuitable as load-bearing implants. Clinically, hydroxyapatite has been used as filler for bone defects and as an implant in load-free anatomic sites (for example, nasal septal bone and middle ear). In addition, hydroxyapatite has been used as a coating on metallic orthopedic and dental implants to promote their fixation in bone. In these cases, the underlying metal carries the load, whereas the surrounding bone strongly bonds to hydroxyapatite. Delamination of the ceramic layer from the metal surface, however, can create serious problems and lead to implant failure.

Table 1.4: Mechanical Properties of Ceramic Biomaterials.

	Young's Modulus (GPa)	Compressive Strength (MPa)	Tensile Strength (MPa)
Alumina	380	4500	350
Bioglass-ceramics	22	500	56–83
56–83Calcium phosphates	40–117	510–896	69–193
Pyrolytic carbon	18–28	517	280–560

1.2.3 Polymeric Biomaterials

Polymers are the most widely used materials in biomedical applications. They are the materials of choice for cardiovascular devices as well as for replacement and augmentation of various soft tissues. Polymers also are used in drug delivery systems, in diagnostic aids, and as a scaffolding material for tissue engineering applications. Examples of current applications include vascular grafts, heart valves, artificial hearts, breast implants, contact lenses, intraocular lenses, components of extracorporeal oxygenators, dialyzers and plasmapheresis units, coatings for pharmaceutical tablets and capsules, sutures, adhesives, and blood substitutes. Examples of polymers and their uses are given in Table 1.5.

Table 1.5: Biomedical Applications of Polymers.

Applications	Polymer(s)
Cardiovascular implants	Polyethylene; poly (vinyl chloride); polyester; silicone rubber; Poly (ethylene terephthalate); polytetrafluoroethylene
Orthopaedic implants	Ultra-high-molecular-weight polyethylene; poly (methyl methacrylate)
Drug release	Poly (lactide-co-glycolide)
Tissue engineering	Poly (lactic acid); poly (glycolic acid); poly (lactide-co-glycolide)

1.2.3.1 Basic Properties of Polymeric Biomaterials

Polymers are organic materials consisting of large macromolecules composed of many repeating units. These long molecules are covalently bonded chains of atoms. Unless they are cross-linked, the macromolecules interact with one another by weak secondary bonds (hydrogen and van der Waals bonds) and by entanglement. Because of the covalent

nature of interatomic bonding within the molecules, the electrons are localized and consequently polymers tend to be poor thermal and electric conductors.

The mechanical and thermal behaviour of polymers is influenced by several factors, including the composition of the backbone and side groups, the structure of the chains and the molecular weight of the molecules. Plastic deformation occurs when the applied mechanical forces cause the macromolecular chains to slide past one another. Changes in polymer composition or structure increase resistance to relative movement of the chains increase the strength and decrease the plasticity of the material. Substitutions into the backbone that increase its rigidity hinder movement of the chains. Bulky side groups also make disentanglement more difficult. Increasing macromolecule length (molecular weight) also makes the chains less mobile and hinders their relative movement.

1.2.3.2 Degradation

Degradation of polymers requires disruption of their macromolecular structure and can occur by either alteration of the covalent interatomic bonds in the chains or alteration of the intermolecular interactions between chains. The former can occur by chain scission (cleavage of chains) or cross-linking (joining together of adjacent chains), an unlikely occurrence under physiological conditions. The latter can occur by incorporation (absorption) or loss (leaching) of low-molecular-weight compounds. For polymers, the method of sterilizing the biomaterial can significantly alter its properties. For example, high temperatures (121–180^0 C), steam, chemicals (ethylene oxide) and radiation can compromise the shape or mechanical properties of polymeric materials.

Polymers may contain various (often unspecified) additives, traces of catalysts, inhibitors and other chemical compounds needed for their synthesis. Over time in the physiological environment, these compounds can leach from the polymer surface. As is the case with corrosion by-products released from metallic implants, the chemicals released from polymers may induce adverse local and systemic host reactions that cause clinical complications. This release is a concern for materials, such as bone cement, that are polymerized in the body and for flexible polymers, such as poly (vinyl chloride), that contain low molecular- weight species (plasticizers) to make them pliable.

In addition to unintentional degradation, certain polymers have been designed to undergo controlled degradation. Among biodegradable polymers, poly (lactic acid), poly (glycolic acid), and their copolymers have been the most widely used. These materials degrade into smaller fragments as well as monomers, such as lactic acid, that can be eliminated by normal metabolic processes of the body. Biodegradable polymers are used for sutures, controlled drug delivery, tissue engineering and fracture fixation.

1.2.3.3 Mechanical Properties

The mechanical properties of polymers depend on several factors, including the composition and structure of the macromolecular chains and their molecular weight [5]. Table 1.6 lists some mechanical properties of selected polymeric biomaterials. Compared with metals and ceramics, polymers have much lower strengths and moduli but they can be deformed to a greater extent before failure. Consequently, polymers are generally not used in biomedical applications that bear loads (such as body weight). Ultra-high-molecular-weight polyethylene is an exception [6], as it is used as a bearing surface in hip and knee replacements. However, the mechanical properties of polymers are sufficient for numerous biomedical applications.

Table 1.6: Mechanical Properties of Polymers

Polymer	Tensile Strength (MPa)	Young's Modulus (GPa)	% Elongation
Poly(methyl methacrylate) (PMMA)	30	2.2	1.4
Nylon 6/6	76	2.8	90
Poly(ethylene terephthalate)	53	2.14	300
Poly(lactic acid)	28-50	1.2-3	2-6
Polypropylene	28-36	1.1-1.55	400-900
Polytetrafluoroethylene	17-28	0.5	120-350
Silicone rubber	2.8	Up to 10	160
Ultra-high-molecular-weight polyethylene (UHMWPE	≥3.5	4-12	≥300

1.3 Biocompatibility studies

For any material to be applied for biotechnological usage, it should pass through a strict regimen of various *in vitro* and *in vivo* tests, which qualify the material as "compatible" with its living" neighbourhood. In other words, when kept in cell culture environment (*in vitro*) or kept in contact with living carriers (tNo.) (*in vivo*), it should not lead to detrimental reactions which change the intrinsic properties (cell growth rate, cell morphology, accumulation of unwanted proteins, overexpression of housekeeping and other genes, denaturation of structural and functional proteins etc.) of the nearby and

distant environment over a period of time. These assessments are done with the help of various techniques some of which are listed below.

1.3.1 In vitro test

Cell count and cell viability study is done by counting cells over a cell counter (Neubar's Chamber) after diluting (1:1) with trypan blue dye. Dead cells immediately take up the dye while living cells start to take up after some time period within which number of viable cells can be counted [7]. Cell viability can also be assessed by MTT (3-(4, 5-Dimethylthiazol-2-yl)-2,5-diphenyltetrazolium bromide) assay in which living cells are differentiated against the dead cells by their capability of metabolizing the chromogen to give blue crystals [8]. Cell morphology can be assessed by observation under high magnification by light microscope and further by electron microscope. The latter can give the idea of surface adherence of cells on the material if the sample is biocompatible (figure 1.1) [9]. Polyacrylamide gel electrophoresis (followed by western blotting, if needed) and fast performance liquid chromatography of the supernatant can give an idea of the changes (both in amount and nature) in the secreted protein profiles [7-9]. Agarose gel electrophoresis (followed by southern/northern blotting, if needed) can show the changes at the nucleic acid level.

1.3.2 In vivo test

Visual evidence of any unwanted tNo. Reaction is the initial "test" done usually. This is followed by taking biopsy of nearby and distal tNo. And performing histopathology (followed by immunohistochemistry, if needed) tests, which qualitatively show the extent/nature of No. Damage.1.1 (a) and (b).

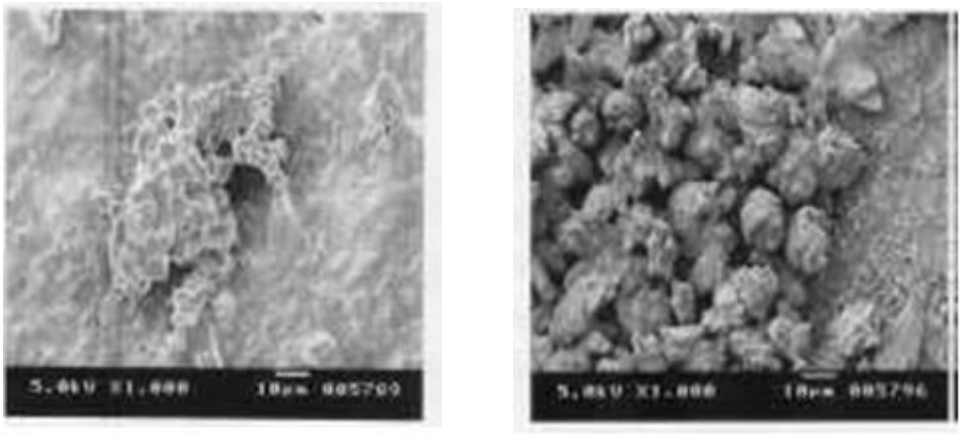

Figure 1.1: SEM photographs of WBC cells grown on magnetic oxide-based glass surface (a) not biocompatible (b) biocompatible [9].

1.4 Selection of Materials for Biomedical Applications

In the past, success of materials in biomedical applications [10] was not so much the outcome of meticulous selection based on biocompatibility criteria but rather the result of serendipity, continuous refinement in fabrication technology and advances in material surface treatment. In the present and future, election of a biomaterial for a specific application must be based on several criteria. The physicochemical properties and durability of the material, the desired function of the prosthesis, the nature of the physiological environment at the organ/tissue level, adverse effects in case of failure, as well as cost and production issues must be considered for each specific application. Biocompatibility is the paramount criterion that must be met by every biomaterial. Mechanical requirements must also be taken into consideration when choosing materials for biomedical applications. Material strength (tensile or compressive), stainless, fatigue endurance, wear resistance, and dimensional stability should be considered with respect to the end use of the prosthetic device to ensure its success. For example, a rigid, strong material would be more suitable for a hip implant, whereas a flexible, less strong material would be sufficient for a vascular graft. Moreover, the performance of materials under dynamic loading conditions must be considered when appropriate, because many implants are subjected to various types and magnitudes of repeated stresses in the body. Consider a hip, knee or ligament replacement that will be subjected to approximately one

million steps per year, while various other physical activities will exert different loads across the joints. At 70 beats per minute, a prosthetic heart valve would experience over three and a half million cycles per year. Other physical properties (such as electrical and thermal conductivity, light transmission and radiopacity) are important for specific applications, such as pacemaker electrodes, intraocular lenses and dental restoratives, and must be considered when applicable. Because the practice of medicine and surgery requires sterile products, decisions regarding choice of biomaterial(s) for a specific application should include consideration of sterilization of the final product(s). Moist heat and high pressure (typical conditions in steam autoclaves), ethylene oxide gas and gamma radiation are procedures commonly used in sterilizing biomedical materials and devices. Special care should be taken with polymers that do not tolerate heat, absorb and subsequently release ethylene oxide (a toxic substance), and degrade when exposed to radiation.

1.5 Biomaterials for Implantable Devices: Present and Future Directions

Unquestionably, important advances have been made in the clinical use of medical implants and other devices. Presently, emphasis is placed on the design of proactive biomaterials, that is, materials that elicit specific, desired and timely responses from surrounding cells and tissues. Medical research continues to explore new scientific frontiers for diagnosing, treating, curing and preventing diseases at the molecular/genetic level. With this new found knowledge, there will be further need for innovative formulations or modifications of existing materials for novel materials and for non-traditional applications of biomaterials, such as in tissue engineering. Promising developments include bio inspired chemical and topographic modifications of materials surfaces, current-conducting polymers and Nano phase materials. In addition to new challenges and opportunities, some of the unresolved issues (primarily, biocompatibility) of the past and present will also need to be addressed in the future.

CHAPTER-2

LITERATURE REVIEW

Bioactive ceramics include bioactive glasses, bioactive glass-ceramics, and dense hydroxyapatite (HA) ceramics. Common feature of these materials is that they bond to bone with no fibrous tissue at the interface. Since the 1970's, when it was first realized that the special properties of ceramic materials could be exploited to provide better materials for certain implant applications, the field has expanded enormously.

The first bioactive material reported, Bioglass 45S5, was four-component silica glass (45 wt % SiO_2, 24.5 wt. % CaO, 24.5 wt. % Na_2O and 6 wt. P_2O_5). The low silica content and the presence of sodium ions in the glass result in very rapid ion exchange with the proton and hydronium ions of physiological solutions [11].

The ion exchange creates and alkaline pH (>7) at the implant interface with the body fluid leading to the nucleation and crystallization of a carbonate apatite layer that is equivalent chemically and structurally to the biological bone mineral [12]. Until the late 1980s, the rapid rate of hydroxyl carbonate apatite (HCA) formation exhibited by the bioglass was attributed to the presence of Na_2O and other alkali and alkaline earth ions in the glass composition. Addition of other multivalent ions such as aluminium or boron stabilized the glass structure (by eliminating non bridging oxygen's) but served to retard the rate of HCA formation [13]. It is now widely accepted that increasing silica content in glass decrease the rate of dissolution. This is due to reduction in the number of network modifier ions present in the glass structure, which serve to disrupt the network resulting in faster network breakdown.

Hench et al. [14] have revealed that for melt-derived bioactive glasses, three key compositional features to these glasses that distinguish them from traditional Na_2O-CaO-SiO_2 glasses and make them highly reactive when exposed to an aqueous medium are:

Less than 60 mol. % silica

High-Na_2O and high-CaO content

High-CaO/P_2O_5.

Glasses with substantially lower molar ratio of Ca to P (in the form of CaO and P_2O_5) do not bond to bone [15]. However, substitutions in the 45S5 formula of 5 to 15 wt. % B_2O_3 for SiO_2 or 12.5 wt. % CaF_2 for CaO or crystallizing the various bioactive glass compositions to form glass ceramics has no measurable effect on the ability of the materials to form a bone bond.

The compositional dependence (in weight %) of bone bonding and soft tissue bonding for the Na_2O-CaO-P_2O_5 -SiO_2 glasses is illustrated in fig. 2.1. All glasses contain a constant 6 wt. % of P_2O_5. Composition in the middle of the diagram (region A) forms a bond with bone. Consequently, region A is termed the bioactive-bone-bonding a boundary. Silica glasses within region B (such as window, bottle, or microscope slide glasses) behave as type 1 nearly cannot make the deals and illicit a fibrous capsule at the implant-tissue interface. Glasses within region C are resorbable and disappear within 10 to 30 days of implantation. Glasses within region D are not technically possible and therefore have not been tested as implants [2].

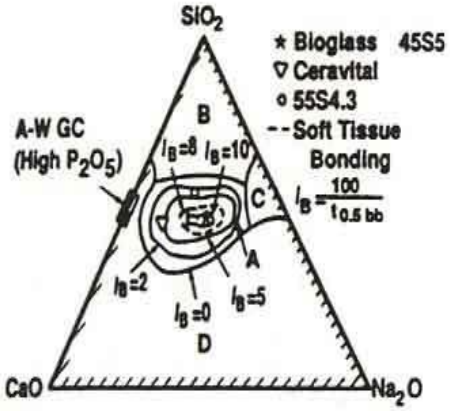

Figure 2.1: Compositional dependence (in weight %) of bone bonding and soft tissue bonding of bioactive glasses and glass-ceramics.

All compositions in region A have a constant 6% of P_2O_5. A/W glass-ceramics has a higher P_2O_5 content. Region E (soft-tissue bonding) is inside the dashed line.

Rajendran et al. [16] made the bioactive glass of composition $53SiO_2–6Na_2O–22CaO–11K_2O–5MgO–2P_2O_5–1B_2O_3$ has been prepared using the melt method. The ultrasonic velocities, attenuation and elastic properties measurements have been made operated at a fundamental frequency of 5MHz at room temperature on bioactive glass before and after different thermal treatment conditions. Thermal treatments of bioactive glasses lead to changes in elastic properties of bioactive glass. Furthermore, a long-term thermal treatment at higher temperatures also seemed to cause such changes to the glass surface that the formation of Ca layer was inhibited during a 48 h immersion in simulated body fluid (SBF).

Vogel and Holand [17] developed the Bioverit family of glass ceramic in which MgO content is in the range 6-28 mol. %. These glass-ceramics have apatite, mica and/or cordierite phases in their structure. Authors have reported a direct intergrowth between the materials and the living tissues. The role of magnesium oxide in glasses and glass-ceramics of the system $CaO-P_2O_5-SiO_2-MgO$ (AI_2O_3) in a pseudo-extracelluar fluid is investigated. They found that ability to form the apatite layer in glass-ceramics decreases with increasing MgO content, so that glass-ceramics with more than 8 wt. % MgO did not form such layer.

Kokubo et al. [18] worked on $SiO_2-CaO-P_2O_5-MgO$ system and developed the A-W.G glass containing (wt. %) 4.6 MgO, 44.7 CaO, 34 SiO_2, 16.2 P_2O_5 and CaF_2. An apatite and wollastonite containing glass ceramic (A-W.GC) was obtained by crystallization of a glass powder compact. They also developed the A.GC and A-W-CP.GC glass ceramics, the first being rich in apatite and the second in apatite, wollastonite and tricalcium phosphate. When in contact with simulated body fluid (SBF) these materials developed an HCA layer with compositional and structural characteristics similar to the one developed on the bioglass surface. Mechanism was proposed to explain the bioactive of these materials based on the ceramic leaching with Ca^{2+} and Si^{4+} dissolution and increase in local fluid supersaturation with respect to apatite, followed by nucleation of apatite on sites of material provided by the dissolution of silicate ions.

El-Egili et al. [19] analysed Infrared spectra of $Na_2O–B_2O_3–SiO_2$ and $Al_2O_3–Na_2O–B_2O_3–SiO_2$ glasses (with intermediate SiO_2 contents) have been to calculate the fraction N4 of four coordinated borons. A reasonable agreement between the N4 values calculated from IR spectra and those determined from NMR spectroscopy (or using literature models) could be attained under certain condition. It has been proposed that the absorption bands in the region 1000–1120 cm^{-1}arise from contributions of SiO_2 and B_2O_3 vibrations the contribution of an oxide is proportional to its concentration. Heat treatment of $Na_2O–B_2O_3–SiO_2$ glasses does not change the value of N4 and this indicates that the structure of alkali borate phase is the same in the glass obtained from melt and in the heat-treated one.

Franks [20] have been developed soluble glasses for biomedical applications containing P_2O_5 as a network former and CaO and Na_2O as modifiers. Study shows that as expected, the glasses have an inverse exponential relationship between solubility and CaO content. Furthermore, there is evidence for compositional related non-linearity in the dissolution of the glasses with time. This is thought to be due to either layer formation on the glass surface hindering ion diffusion, ion exchange process or change of ionic strength of the solution. Bioactivity of these glasses is indicated by the formation of a brushite precipitate, a precursor to apatite formation.

Jalota et al. [21] A Tris–HCl-buffered synthetic body fluid (SBF) solution, mimicking the human blood plasma, with the following ion concentrations of 27 mM HCO^{3-}, 2.5 mM Ca^{2+}, 1.0 mM HPO_4^{2-}, 142 mM Na^+, 125 mM $Cl^–$, 5 mM K^+, 1.5 mM Mg^{2+}, and 0.5 mM SO_4^{2-} was used as an aqueous medium to process a number of bone substitute materials under the so-called biomimetic conditions of 37 °C and pH 7.4. This solution was named as Tris–SBF-27 mM. Firstly, collagen sponges were soaked in Tris–SBF-27 mM solution at 37 °C and were found to be fully covered with nanoporous apatitic calcium phosphate (Ap-CaP). The composites of collagen–Ap-CaP biomaterials are expected to be used in orthopedic and dental surgery. Secondly, Ap-CaP short whiskers or microrods with a novel nanotexture and surface areas higher than 45 m^2/g were synthesized in Tris–SBF-27 mM solution. Thirdly, calcium sulfate cements doped with $CaHPO_4$ (monetite), were shown to have apatite-inducing ability upon ageing in Tris–SBF-27 mM. $CaHPO_4$

addition in calcium sulfate was found to improve its mechanical strength, measured after cement setting reaction. Pure calcium sulfate cement pellets were not stable in Tris–SBF-27 mM solutions and crumbled into a powder. All the samples were characterized by SEM, XRD, FTIR, surface area and mechanical strength measurements. Macroporous collagen sponges were biomimetically coated with carbonated, apatitic calcium phosphate (Ap-CaP) by using the above-mentioned Tris–SBF- 27 mM solution at 37 °C and pH 7.4. Short whiskers or microrods of apatitic CaP were converted to high surface area, biomimetic CaP microrods by soaking crystalline CaP precursors of rod-like morphology in Tris–SBF-27 mM solution at 37 °C.

Xin et al. [22] have reported the formation of calcium phosphate (Ca-P) on various bioceramic surfaces in simulated body fluid (SBF) and in rabbit muscle sites was investigated. The bioceramics were sintered porous solids, including bioglass, glass-ceramic hydroxyapatite, a-tricalcium phosphate and b-tricalcium phosphate. The ability of inducing Ca-P formation was compared among the bioceramics. The Ca-P crystal structures were identified using single-crystal diffraction patterns in transmission electron microscopy. The examination results show that ability of inducing Ca-P formation in SBF was similar among bioceramics, but considerably varied among bioceramics in vivo. Sintered b-tricalcium phosphate exhibited a poor ability of inducing Ca-P formation both in vitro and in vivo. Octacalcium phosphate (OCP) formed on the surfaces of bioglass, A-W, hydroxyapatite and a-tricalcium phosphate in vitro and in vivo.

Oliiverira et al. [23] have prepared the glass and glass ceramic of MgO-CaO- P_2O_5- SiO_2 glass for different compositions. The Ca/P rich layer has been identified as hydroxyapatite on both samples after immersion in SBF for different time periods but the precipitated film on glassy sample was weakly bonded and the glass ceramic was strongly adhesive. These microstructural characteristic has been observed through SEM studies. Although, the glass ceramic has higher chemical and mechanical stability, these glasses are expected to be capable of bone boding with bone which results in good bioactivity.

Simon et al. [24] the in vitro behaviour of xAg_2O $(100 - x)$ $[50P_2O_5$-30CaO- $20Na_2O]$ glasses (0.14 x 20 mol %) is investigated in simulated body fluid (SBF) mainly with

respect to bioactivity and silver ions release. In order to estimate the biodegradability and bioactivity, the samples were soaked in SBF, which has almost equal ions concentration to those of human blood plasma, and kept at 37 ^{0}C for fixed periods of time up to 18 days. After the fixed periods of time analyses were performed on the SBF solutions. Calcium and silver ions concentration of SBF after different soaking times of the glass samples were primarily examined. Conductivity data support the assumption that the released silver ions are reduced in SBF and their release is obstructed by growth of the bioactive layer on the glass surface. X-ray diffraction and infrared analysis attest the development on glass surface of a hydroxyapatite type layer.

Rapacz et al. [25] has reported the performance of hydroxyapatite material in a living body depends on a number of factors. Stability of hydroxyapatite structure, which is influenced by both, preparation conditions of the starting precursor powders and fabrication method of the implant materials, is an important one. Inappropriate preparation conditions of synthesis, calcination of powder and sintering of formed samples result in dehydroxylation and even in decomposition of HAP which lead to the change in the physicochemical properties of implants. In the work samples of hydroxyapatite ceramics have been obtained by two methods, i.e. by hot pressing and by pressure less sintering in the temperature range of 1150–1300 °C. The materials prepared have been studied using FTIR and XRD in order to identify the dehydroxylation processes and the possible hydroxyapatite decomposition during thermal treatment. The usefulness of both methods in identification of thermal stability of hydroxyapatite was confirmed. In early 1990s, sol-gel processing was introduced for the synthesis of bioactive glasses. The sol-gel route allows glasses of higher purity and homogeneity to be obtained at temperatures notably lower than those required to obtain glasses by the melting method. These bioactive glasses have higher bioactivity and reabsorb ability in vitro, which have application as bone graft material. Various research groups used sol-gel route for preparation of bioactive glasses not only in the ternary SiO_2-CaO-P_2O_5 system but also in the quaternary SiO_2-CaO-P_2O_5-MgO system and binary SiO_2-CaO system for biomedical applications. In vitro studies have shown that nucleation and crystallization rates of hydroxycarbonate apatite (HCA) depend on many factors including the sol-gel

glass composition. In the recent time borate glasses have fetched lots of attention for the medical applications.

Kim and Jee [26] have studied the dependence of hydroxyapatite forming behaviour with respect to the crystalline phases in the alumina coated bioactive glasses. When bioactive glazed alumina reacts in the SBF, it is inferred that no silica rich layer has been found in crystallized bioactive glazed alumina, while Si-rich layer has been formed on the bioactive bulk glass. Glass ceramics containing magnetic phase with glass matrix, could be used as thermo seed for hyperthermia treatment of cancer [27]. This magnetic phase is exposed to alternating magnetic field, by which heat is generated due to hysteresis loss. This hyperthermia treatment is considered to be an effective treatment for cancer without side effects and this process can be repeated many times after implanting a bioactive and biocompatible ceramic in to the body. A glass ceramic with lithium ferrite ($LiFe_5O_8$) and magnetite (Fe_3O_4) in an AI_2O_3-SiO_2-P_2O_5 glassy matrix could be used as a thermo seed for hyperthermia treatment of cancer.

Roman et al. [28] studied the influence of the phosphorus on the crystallization and bioactivity of glass-ceramics obtained from sol–gel glasses. For this purpose two sol–gel glasses with a similar composition but one of them containing P_2O_5 (70% SiO_2; 30% CaO and 70% SiO_2; 26% CaO; 4% P_2O_5, mol %) were prepared. Pieces of these glasses were treated at temperatures ranging between 700°C and 1400°C for 3 h. The obtained materials were characterized by XRD, FTIR, SEM-EDS and the biaxial flexural strength was determined in samples heated at 1100°C. In addition, an in vitro bioactivity study in simulated body fluid (SBF) was carried out. The results showed that phosphorus plays an important role in the crystallization of the glasses: it induced the crystallization of calcium phosphate phases, the stabilization of the wollastonite phase at high temperature as well as the crystallization of SiO_2 phases at low temperatures. Moreover, the presence of phosphorus produced a heterogeneous distribution of defects in the pieces and, therefore, the flexural strength of samples containing this element decreased. Finally, glass ceramics obtained from glasses containing phosphorus showed the fastest formation rate of the apatite layer when soaked in SBF.

Sanz-Herrera et al. [29] have studied that the evaluation of the degradation of bioactive glasses in contact with body fluid requires long-term in vitro assays. In his work, a novel mathematical model is proposed to numerically analyse the dissolution and bioactivity of bioactive glasses in relevant conditions for their in vitro and in vivo applications. A detailed framework is described for the numerical implementation using the Voxel-FEM method, in order to account for the microstructural evolution as consequence of degradation and HA layer formation. Two examples of application are highlighted, showing the suitability and usefulness of the proposed model for the evaluation of bioactive glasses in tissue engineering applications.

Saravanakumar et al. [30] have studied the impact of nanotechnology in biomaterials is of interest because of the enhancement in their biocompatibility and bioactivity. In this investigation, the preparation of nanobioactive glasses by using different methods (such as sol–gel, hydrothermal and sonochemical) is discussed in detail. The structural and morphological characterisation of the prepared samples was made. The silica-based nanobioactive glasses (NBG) with a composition of $48SiO_2$–$40CaO$–$12P_2O_5$ were prepared by three different methods, namely sol–gel, hydrothermal and sonochemical. The different characterisation studies on NBGs reveal a higher bioactivity in SCP-3(sol-gel method) than other glasses such as SCP-1 (sonochemical method) and SCP-2 (hydrothermal). The higher bone-bonding ability of the NBG that is observed indicates that the sol–gel method is more suitable for the preparation of bioactive glass for implant applications.

Goudouria [31] studied that modification of a widely used dental ceramic by a bioactive glass via sol–gel method resulted in the fabrication of novel dental ceramic composites with bioactive behaviour. The presence of leucite (Lt), apatite (Ap), various calcium silicate phases (CS) and a glassy alumina silicate matrix were detected, while after sintering the predominance of wollastonite (W) among the other calcium silicate phases was observed, along with further crystallization of apatite. Concerning the bioactivity, the onset of the apatite formation was directly dependent on the bioactive glass amount, while a delay of the sintered specimens compared to the raw powders was also observed.

Cannillo et al. [32] investigated ceramics have the ability to form direct bonds with surrounding tissues when implanted in the body. Among bioactive ceramics, the apatite/wollastonite (A/W) glass–ceramic, containing apatite and wollastonite crystals in the glassy matrix, has been largely studied because of good bioactivity and used in some fields of medicine, especially in orthopedics and dentistry. However, medical applications of bioceramics are limited to non-load bearing applications because of their poor mechanical properties. In this study, A/W powders, obtained from industrial and high grade quality raw materials, were thermally sprayed by APS (atmospheric plasma spraying) on Ti–6Al–4V substrates, in order to combine the good bioactivity of the bioceramic and the good mechanical strength of the titanium alloy base material. The microstructure and the resulting properties were evaluated depending on processing parameters and post-processing thermal treatments. The morphology and the microstructure of the coatings were observed by SEM and the phase composition was examined by X-ray diffraction [33]. The bioactivity of the coatings was evaluated by soaking the samples in a simulated body fluid (SBF) for 1, 2 and 5 weeks. The bioactive behavior was then correlated with the thermal treatments and the presence of impurities (in particular Al_2O_3) in the coatings. The results of the present bioactivity study demonstrated that the as-sprayed AWC and AWP coatings were bioactive materials and the bioactive mechanism of these as sprayed coatings was similar to that of bioactive glasses as proposed by Hench. Moreover, the bioactivity of the AWC and AWP glass–ceramic coatings depended mainly on the amount of the glassy matrix and the amount of Al_2O_3 in the composition.

Peitl et al. [34] have shown that crystallization of Bioglass 45S5 did not inhibit HCA formation in an invitro test with SBF-K9 even with a fully crystallized glass-ceramic. The onset time for HCA layer formation did decrease with increased crystalline in his study. They concluded a fact that crystallization did not affect significantly the kinetic reactions in 1.5 Na_2O-1.5 CaO-3 SiO_2 containing 0, 2, 4, 6, wt. % P_2O_5 glasses. This system of glasses was shown to be highly bioactive as these show bioactivity even in the absence of phosphorous than other commercial bioactive glass-ceramics. They have revealed the in vitro bioactivity of partially crystallized 45S5 bioglass as a function of time through in situ observation using AFM. The thermal treatments have been carried out to obtain a

material that is less resorbable, still bioactive and stiffer than standard bio-glass. This crystallized bioglass is more suitable than those of hydroxyapatite faces and can be used as filler for polymeric matrix bioactive composite.

Chen et al. [35] established the sol–gel process of producing SiO_2–CaO bioactive glasses, but problems remain with the poor mechanical properties of the amorphous form and the bioinertness of its crystalline counterpart. These properties may be improved by incorporating Na_2O into bioactive glasses, which can result in the formation of a hard yet biodegradable crystalline phase from bioactive glasses when sintered. However, production of Na_2O-containing bioactive glasses by sol–gel methods has proved to be difficult. This work reports a new sol–gel process for the production of Na_2O-containing bioactive glass ceramics, potentially enabling their use as medical implantation materials. The first time fine powders of 45S5 (a Na_2O-containing composition) glass ceramic have been successfully synthesized using the sol–gel technique in aqueous solution under ambient conditions. A comparative study of sol–gel derived S70C30 (a Na_2O-free composition) and 45S5 glass ceramic materials revealed that the latter possesses a number of features desirable in biomaterials used for bone tissue engineering, including (i) the crystalline phase $Na_2Ca_2Si_3O_9$ that couples good mechanical strength with satisfactory biodegradability, (ii) formation of hydroxyapatite, which may promote good bone bonding. In contrast, the sol–gel derived S70C30 glass ceramic consisted of a virtually inert crystalline phase $CaSiO_3$. Moreover, amorphous S70C30 largely transited to $CaCO_3$ with minor hydroxyapatite when immersed in simulated body fluid under standard tissue culture conditions. In conclusion, sol–gel derived Na_2O-containing glass ceramics have significant advantages over related Na_2O free materials, having a greatly improved combination of mechanical capability and biological absorbability. Novel bioactive sol–gel derived dental bioactive glass/dental ceramic (BG/DC) glass–ceramic composites with various ratios of DC were fabricated. The in vitro biological response of all composites up to 40% of DC followed an inversely linear relationship with the amount of DC, while the composite with 50% of DC is proven non-bioactive. The results of this study suggest that the use of the sol–gel process is an acceptable alternate method for the fabrication of bioactive dental glass ceramic materials. However mechanical properties

evaluation and the biodegradation as well as the in vitro biological behaviour of the fabricated materials should confirm their future use in clinical applications.

Liu [36] studied in order to improve the bioactivity of the micro-arc oxidized magnesium, a calcium phosphate coating was formed on the surface of micro-arc oxidized magnesium using a chemical method. The microstructures of the substrate and the calcium phosphate coating before and after the simulated body fluids (SBF) incubation were characterized by X-ray diffraction, Fourier-transformed infrared spectroscopy and scanning electron microscopy. The results showed that the calcified coating was composed of calcium deficient hydroxyapatite (HA) and dicalcium phosphates dehydrate (DCPD). After SBF incubation, some new apatite formation on the calcified coating surface from SBF could be found. The corrosion behaviors of the samples in SBF were also investigated by potentiodynamic polarization curves and immersion tests. The results showed that calcium phosphate coating increased the corrosion potential, and decreased the hydrogen gas release.

Hashizume [37] studied preparation of colloidal hydroxyapatite (HAp) particles under body fluid conditions was investigated with focusing on the effect of preparative conditions on crystallinity of the resulting particles. Tris(hydroxymethyl)aminomethane was added to 1.5SBF (a solution having 1.5 times higher ion concentrations than those of a simulated body fluid, SBF) to increase the solution pH, which resulted in induction of homogeneous nucleation of HAp in the solution. Colloidal HAp particles having diameters about 300nm were obtained. When the reaction was preceded at 70 °C and the sample was dried by heating, it was effective to obtain HAp particles having high crystallinity. Experimental results support that remaining water in the sample contributed to increase HAp crystallinity.

Nayak [38] SiO_2–Na_2O–CaO based bioglass-ceramics was synthesized through sol–gel route using rice husk ash as silica source. The decomposition behavior of gel was evaluated. Sodium–calcium–silicate phases were crystallized above 700 °C. Pellet made of glass-ceramics powder was sintered at 900 °C. In vitro bioactivity and biodegradability of glass-ceramics were investigated by incubation in simulated body fluid and Tris buffer solution respectively. Scanning electron microscopy, energy dispersive spectroscopy and

X-ray diffraction were used to monitor the surface deposition on glass-ceramics during incubation. The material showed a good bioactivity with a formation of carbonated hydroxy apatite phase in 3 days of incubation. A quick degradation of the material was observed in Tris solution associated with an increase of pH due to the dissolution of Ca^{2+} and Na^{+} ionic species. All these results suggest the glass-ceramics, prepared utilizing rice husk ash, would be a low cost biomaterial for potential biomedical applications.

CHAPTER-3

PROPOSED-WORK AND EXPERIMENTAL TECHNIQUES

The detail about sample processing methodology, which was followed during the course of the investigation, is presented in this chapter. The detailed measurement techniques and procedure employed for in vitro bioactivity testing, density, X-ray diffraction (XRD), band gap measurement of samples by UV-Visible Spectroscopy and Fourier transform infrared spectroscopy (FTIR) are given in details.

3.1 Sample Preparation

Glass composition is given in table 3.1 these composition were prepared by grinding the raw materials using conventional techniques followed by melting. Each batch was prepared by taking an appropriate mole fraction of well-desired initial ingredients and grinding them in mortar and pestle.

Table 3.1: Glass compositions (mol %) with their label.

Glass Label	SiO_2	Al_2O_3	TiO_2	CaO	Na_2O
G 2	60	10	5	15	10
G 3	55	10	5	15	15
G 4	50	10	5	15	20

For each system, required amount of raw materials as per the stoichiometry ratio was taken. The mixture was grind to break agglomerate particles. After grinding, the mixture was further transformed to ball mill and ground for two hours in a ball mill in dry medium. The ball milling was done using agate balls in agate jar (Retsch, Germany, Model PM 100). The mass to ball ratio for each system was 1:2 which was kept constant for each milling. The mixed dried powder of the homogenous mass was transformed in recrystallized alumina crucible. The powder of the samples was initially heated to achieve a temperature of 1000ºC in 2 hrs. The temperature was maintained at 1000^{o}C for 30 minutes to facilitate the calcination. During heating process moisture is released and the calcinations occur. After that the temperature was increased up to 1200^{o}C and kept at this temperature for 30 minutes to facilitate the fusion and melting process. Then, system was reheated at 1500ºC and kept at this temperature for 1 hour 45 minutes in order to achieve the homogeneous molten glass. The melt was poured on the flat copper plate and quenched by other copper plate in air to obtain flakes. All the samples were prepared using the same route as described above.

3.1.1 Annealing

The obtained frits were annealed at 500^{o}C (below T_g, transition temperature) for 10 hours in air in a calibrated resistance heating furnace. The annealing process is done to remove the internal stresses generated during quenching process.

3.2 SBF solution and In-Vito test

Kokubo and his colleagues developed a cellular simulated body fluid that has inorganic ion concentrations similar to those of human extracellular fluid, in order to reproduce formation of apatite on bioactive materials *in vitro*. This fluid can be used for not only evaluation of bioactivity of artificial materials *in vitro*, but also coating of apatite on various materials under biomimetic conditions. The ion concentrations of SBF are given on Table 3.1 [32]

Table 3.2: Ion concentrations of the simulated body fluid and human blood plasma

Ion	Simulated body fluid	Human blood plasma
Na^+	142.0	142.0
K^+	5.0	5.0
Mg^+	1.5	1.5
Ca^{2+}	2.5	2.5
Cl^-	147.8	103.0
HCO_3^-	4.2	27.0
HPO_4^{2-}	1.0	110
SO_4^{2-}	0.5	0.5

The pH of SBF was adjusted to pH 7.25 at 36.5^{o}C, by using 50 mM (mol/dm^3) of tris (hydroxymethyl) aminomethane and approximately 45 mM of HCl. When apatite-forming ability of the specimen is not so high, pH of SBF is sometimes adjusted to pH 7.40.

3.3 PREPARATION OF SBF

SBF is a metastable solution containing calcium and phosphate ions already supersaturated with respect to the apatite [39]. The details of SBF preparation is given in the following section:

3.3.1 Cleaning

Clean all the bottles including flasks, beakers etc. with dilute hydrochloric acid solution, sterilizing agent and ultra-pure water in this order

Immerse all the bottles etc. in dilute hydrochloric acid solution for several hours. Remove the bottles from the solution and wash with tap water well.

Immerse the bottles etc. in sterilizing liquid for overnight. Remove them from the liquid, and washed with ultra-pure water well.

Wash the bottles with ion-exchanged water for several times and cover their mouths with wrapping film. The bottles do not need to be dried. If the bottles would need to be dried place them in drier below 50^{o}C.

3.3.2 Dissolution of chemicals

Put 750 ml (=cm^3) of ultra-pure water into a 1000 ml beaker (polyethylene beaker is preferred). Stir the water and keep its temperature at 36.5 $^{\circ}$C with magnetic stir with heater. The beaker is preferred to be placed in clean bench, to avoid dusts.

Add each chemical into the water until, one by one, after each reagent was completely dissolved. Weigh a chemical with weighing bottle. Add it in the water. Wash the remaining chemical on the weighing bottle with ultra-pure water and add the solution in the water.

Addition of reagent should be little by little with less than about 1g, in order to avoid local increase in pH of the solution.

3.3.3 Adjustment of pH

Calibrate the pH meter with fresh standard buffer solution.

7After, check the temperature of the solution in the beaker, and place the electrode pH meter in the solution. Measure its pH while the temperature is at 36.5 $^{\circ}$C. At this point, pH of the solution is approximately 7.5. Titrate 1kmol/dm^3-HCl solution with pipette to adjust the pH at 7.25 (or 7.40).

After the adjustment of pH, transfer the solution from the beaker to a glass volumetric flask of 1000 ml. Wash the inside of the beaker with ultra-pure water several times and add the solution to the flask.

Add ultra-pure water to the solution, adjusting the total volume of the solution to 1000 ml, and the shake the flask well. Keep the flask at room temperature until its temperature should be approximately 20^{o}C. After cooling, add ultra-pure water again, the solution to the total volume of the solution to 1000 ml, and then shake the flask well.

3.3.4 Storage

Rinse a polyethylene (or polystyrene) bottle of 1000 ml with a bit of the prepared solution (SBF), at least three times. Transfer the solution from the flask to the polyethylene bottle.

Store the bottle in a refrigerator at 5-10 ^{o}C [21].

3.4 CHARACTERIZATION TECHNIQUES

3.4.1 Density and molar volume

The density of glass samples at room temperature was measured by the Archimedes principle. The molar volume (V_m), excess volume (V_e) and oxygen molar volume (V_o) of the glasses will be calculated using the following equation:

$$V_m = M/\rho \qquad (1)$$

where M denotes the molar mass of subjected glass.

$$V_e = V_m \sum X_i V_m(i) \qquad (2)$$

Here, $V_m(i)$ is the molar volume of each oxide constituent X_i is the molar concentration of every oxide in the glass composition. Oxygen molar content in the glasses was calculated using Eq. given below. M_i and X_i is the molar weight of the oxide and oxygen content in the i^{th} oxide [39- 41].

$$V_o = \sum X_i M_i / \rho \sum n_i X_i \qquad (3)$$

3.4.2 Fourier Transform Infra-Red spectroscopy (FTIR)

FITR is very useful technique to access the formation of the Hydroxyapatite layer on the surface of the glasses after dipping in SBF solution. In this technique, the FTIR spectra of

original glass and soaked glass will be taken to compare the any change after dipping in SBF solution. The technical details of this technique are as follows:

In infrared spectroscopy, IR radiation is passed through a prepared sample. Some of the infrared radiation is absorbed by the sample and some of it is passed through (transmitted). The resulting spectrum represents the molecular absorption and transmission, creating a molecular fingerprint of the sample. Like a fingerprint no two unique molecular structures produce the same infrared spectrum. This makes infrared spectroscopy useful for several types of analysis. It can identify their functional groups and their attachment with other groups.

(a) The Analysis Process

The normal instrumental process is as follows:

1. Source: Infrared energy is emitted from a glowing black-body source. This beam passes through an aperture which controls the amount of energy presented to the sample (and, ultimately, to the detector).

2. Interferometer: The beam enters the interferometer where the "spectral encoding" takes place. The resulting interferogram signal then exits the interferometer.

3. Sample: The beam enters the sample compartment where it is transmitted through or reflected off of the surface of the sample, depending on the type of analysis being accomplished. This is where specific frequencies of energy, which are uniquely characteristic of the sample, are absorbed.

4. Detector: The beam finally passes to the detector for final measurement. The detectors used are specially designed to measure the special interferogram signal.

5. The Computer: The measured signal is digitized and sent to the computer where the Fourier transformation takes place. The final infrared spectrum is then presented to the user for interpretation and any further manipulation.

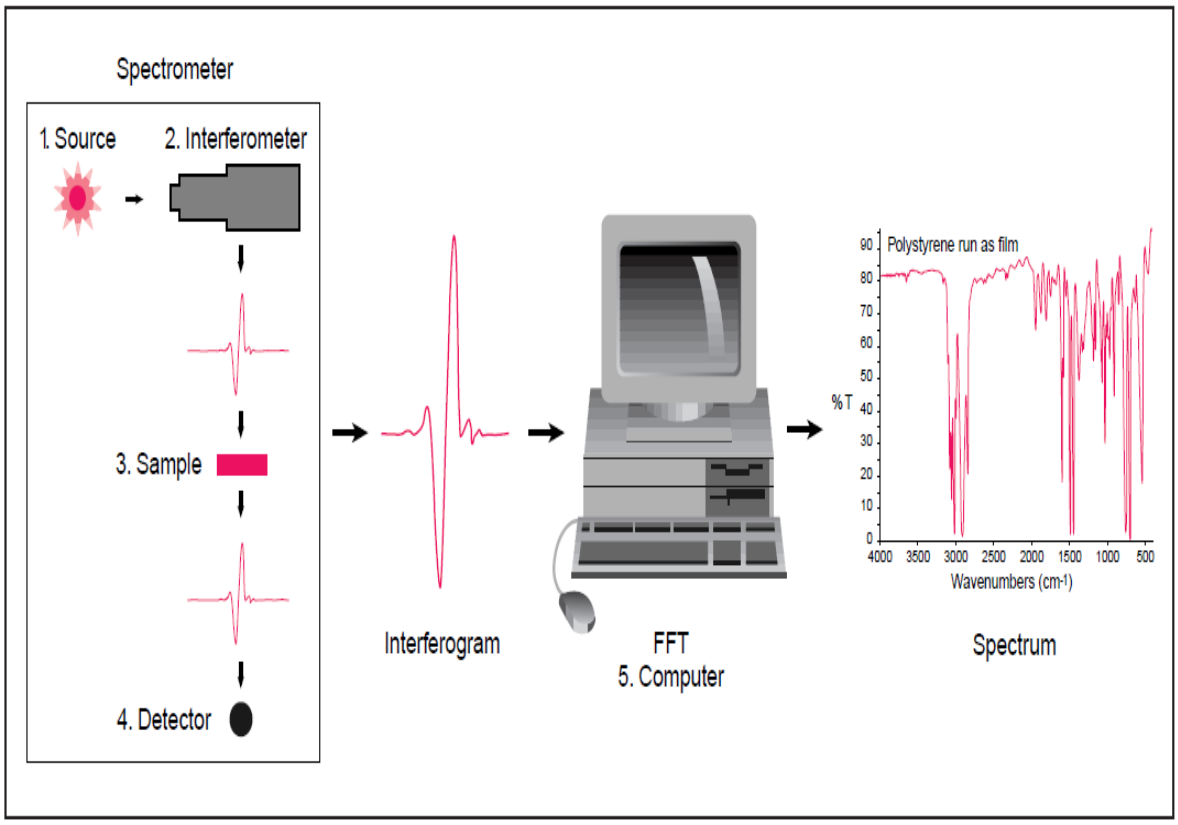

Figure 3.2: Sample analysis process by FTIR.

Because there needs to be a relative scale for the absorption intensity, a background spectrum must also be measured. This is normally a measurement with no sample in the beam. This can be compared to the measurement with the sample in the beam to determine the "percent transmittance."

This technique results in a spectrum which has all of the instrumental characteristics removed. Thus, all spectral features which are present are strictly due to the sample. A single background measurement can be used for many sample measurements because this spectrum is characteristic of the instrument itself.

(b) Advantages of FT-IR

Some of the major advantages of FT-IR over the dispersive technique include:

• **Speed:** Because all of the frequencies are measured simultaneously, most measurements by FT-IR are made in a matter of seconds rather than several minutes. This is sometimes referred to as the Felgett Advantage.

• **Sensitivity:** Sensitivity is dramatically improved with FT-IR for many reasons. The detectors employed are much more sensitive, the optical throughput is much higher (referred to as the Jacquinot Advantage) which results in much lower noise levels, and the fast scans enable the co-addition of several scans in order to reduce the random measurement noise to any desired level (referred to as signal averaging).

• **Mechanical Simplicity:** The moving mirror in the interferometer is the only continuously moving part in the instrument. Thus, there is very little possibility of mechanical breakdown.

• **Presence of internally Calibration:** These instruments employ a He-Ne laser as an internal wavelength calibration standard (referred to as the Connes Advantage). These instruments are self-calibrating and never need to be calibrated by the user.

These advantages, along with several others, make measurements made by FT-IR extremely accurate and reproducible. Thus, it is a very reliable technique for positive identification of virtually any sample. The sensitivity benefits enable identification of even the smallest of contaminants. This makes FT-IR an invaluable tool for quality control or quality assurance applications whether it be batch-to-batch comparisons to quality standards or analysis of an unknown contaminant. In addition, the sensitivity and accuracy of FT-IR detectors, along with a wide variety of software algorithms, have dramatically increased the practical use of infrared for quantitative analysis. Quantitative methods can be easily developed and calibrated and can be incorporated into simple procedures for routine analysis.

Thus, the Fourier Transform Infrared (FT-IR) technique has brought significant practical advantages to infrared spectroscopy. It has made possible the development of many new sampling techniques which were designed to tackle challenging problems which were impossible by older technology. It has made the use of infrared analysis virtually limitless.

3.4.3 X-Ray Diffraction Studies (XRD)

X-ray diffraction is the most wide spread technique for determining the phase identification, crystal structure, lattice parameter of the crystalline solids. A typical powder XRD instrumentation consist of four main components such as X-ray source, specimen stage, receiving optics and X-ray detector. The source and detector with its associated optics lie on the circumference of focusing circle and the sample stage at the centre of the circle. The angle between the plane of the specimen and the X-ray source is θ, known as Bragg's angle and the angle between the projection of X-ray and the detector is 2θ. For the XRD analysis, fine powder samples were mounted on the sample holder and the powder was assumed to consist of randomly oriented crystallites. When a beam of X-ray is incident on the sample, X-rays are scattered by each atom in the sample. If the scattered beams are in phase, these interfere constructively and one gets the intensity maximum at that particular angle. The atomic planes from where the X-rays are scattered are referred to as 'reflecting planes'.

The Bragg's law relates the wavelength (λ) of the X-ray reflected the spacing between the atomic planes (d) and the angle of diffraction (θ) as follows:

$$2d \sin \theta = n \lambda$$

For the first order diffraction, n=1, and knowing θ and λ, one can calculate the interplanar spacing d–value for a particular plane. After recording the X-ray diffraction pattern, first step involves the indexing of XRD peaks. The indexing means assigning the correct Miller indices to each peak of the diffraction pattern. The correct indexing is done only when all the peaks in the diffraction pattern are accounted for the process. There are three main methods for indexing a diffraction pattern:

(i) Comparing the measured XRD pattern with the standard data base (JCPDS cards)

(ii) Analytical methods

(iii) Graphical methods.

In case of fine particles, with reduction in the size of the particles, the XRD lines get broadened, which indicates clearly that particle size has been reduced. Information of the particle size is obtained from the full width at half maximum (FWHMs) of the diffraction peaks. The FWHMs (β) can be expressed as a linear combination of the contributions from the strain (ε) and particle size (L) through the following relation:

$$\text{Cos } \theta/\lambda = 1/L + \varepsilon \text{ Sin } \theta/\lambda$$

3.4.4 Strengths and Limitations of X-ray Powder Diffraction (XRD)

(a) Strengths

Powerful and rapid (< 20 min) technique for identification of an unknown mineral

In most cases, it provides an unambiguous mineral determination

Minimal sample preparation is required

XRD units are widely available

Data interpretation is relatively straight forward

(b) Limitations

Homogeneous and single phase material is best for identification of an unknown

Must have access to a standard reference file of inorganic compounds (d-spacing's, hkls)

Requires tenths of a gram of material which must be ground into a powder

For mixed materials, detection limit is ~ 2% of sample

For unit cell determinations, indexing of patterns for non-isometric crystal systems is complicated

Peak overlay may occur and worsens for high angle 'reflections.'

3.4.5 UV/Visible Spectroscopy

When a sample of an unknown compound is exposed to light, certain functional groups within the molecule absorb UV light of different wavelengths. In UV/Visible spectroscopy, the term chromophore is used to indicate a functional group that absorbs electromagnetic radiation, usually in the UV or visible region. The type of functional groups that absorb ultraviolet light can be conjugated species, such as alkenes, aromatics, etc., making UV/Visible spectroscopy useful for distinguishing conjugated dienes from conjugated trines, and so forth. Also many metal-ligand complexes also absorb UV/visible light. It's important to remember that UV/visible EM radiation causes electronic transitions within a molecule, promoting bonding and non-bonding electrons to higher, less stable anti bonding orbitals. The molecule then loses this excess energy by rotation and vibrational relaxation, but some compounds can lose their energy by emission processes such as fluorescence.

Ultraviolet spectrometers consist of a light source, reference and sample beams, a monochromatic and a detector. The ultraviolet spectrum for a compound is obtained by exposing a sample of the compound to ultraviolet light from a light source, such as a Xenon lamp.

The reference beam in the spectrometer travels from the light source to the detector without interacting with the sample. The sample beam interacts with the sample exposing it to ultraviolet light of continuously changing wavelength. When the emitted wavelength corresponds to the energy level which promotes an electron to a higher molecular orbital, energy is absorbed. The detector records the ratio between reference and sample beam intensities (I/I_o). At the wavelength where the sample absorbs a large amount of light, the detector receives a very weak sample beam. Once intensity data has been collected by the spectrometer, it is sent to the computer as a ratio of reference beam and sample beam intensities. The computer determines at what wavelength the sample absorbed a large amount of ultraviolet light by scanning for the largest gap between the two beams.

When a large gap between intensities is found, where the sample beam intensity is significantly weaker than the reference beam, the computer plots this wavelength as

having the highest ultraviolet light absorbance when it prepares the ultraviolet absorbance spectrum.

3.4. Scanning Electron Microscopy/ Energy Dispersive Spectrometer

A scanning electron microscope (SEM) images a sample by scanning it with a high-energy beam of electrons in a raster scan pattern. The electrons interact with the atoms that make up the sample producing signals that contain information about the sample's surface topography, composition, and other properties such as electrical conductivity.

The types of signals produced by an SEM include secondary electrons, back-scattered electrons (BSE), characteristic X-rays, light, specimen current and transmitted electrons. Secondary electron detectors are common in all SEMs, but it is rare that a single machine would have detectors for all possible signals. The signals result from interactions of the electron beam with atoms at or near the surface of the sample. In the most common or standard detection mode, secondary electron imaging or SEI, the SEM can produce very high-resolution images of a sample surface, revealing details less than 1 nm in size. Due to the very narrow electron beam, SEM micrographs have a large depth of field yielding a characteristic three-dimensional appearance useful for understanding the surface structure of a sample. This is exemplified by the micrograph of pollen shown to the right. A wide range of magnifications is possible, from about 10 times (about equivalent to that of a powerful hand-lens) to more than 500,000 times, about 250 times the magnification limit of the best light microscopes. Back-scattered electrons (BSE) are beam electrons that are reflected from the sample by elastic scattering. BSE are often used in analytical SEM along with the spectra made from the characteristic X-rays. Because the intensity of the BSE signal is strongly related to the atomic number (Z) of the specimen, BSE images can provide information about the distribution of different elements in the sample. For the same reason, BSE imaging can image colloidal gold immuno-labels of 5 or 10 nm diameter which would otherwise be difficult or impossible to detect in secondary electron images in biological specimens. Characteristic X-rays are emitted when the electron beam removes an inner shell electron from the sample, causing a higher energy electron to fill the shell and release energy. In addition to high magnification imaging the SEM

has analysis instrumentation known as Energy Dispersive Spectrometer (EDS), which allow analysis of an area of approximately 1um in diameter. These characteristic X-rays are used to identify the composition and measure the abundance of elements in the sample. This allows analysis of phase boundaries, surface imperfections, comparison of different areas of the sample etc.

4.1 pH measurement

The mechanism and kinetics of hydroxyapatite (HA) precipitation depends on the pH value of the SBF Solution. The change in pH of the SBF is a function of immersion time is depicted in fig. 4.1. The pH value could not show any drastic change with respect to immersion time. However, initially the pH values decrease up to 225 hrs of dipping. Later stages of soaking, the pH values fluctuate between 7.0 to 6.3.

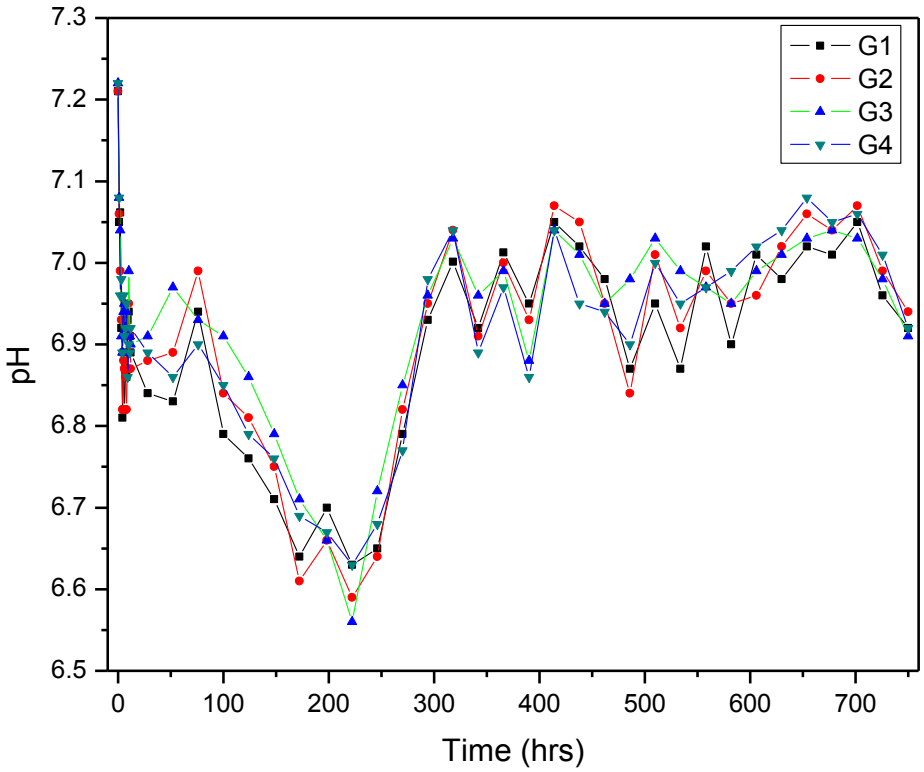

Figure 4.1: Variation of pH in SBF with immersion time.

The species such as $H^{+}_{3}O^{+}$ and OH^{-} from the solution attack the glass network and are exchanged with Ca^{2+}/ Na^{+} ions from the glass network. Leaching of alkaline/ alkali ions from glass to SBF solution leads to increment in pH values. Initial increment in pH

values in glass may be due to release of sodium ions (Na^+) during initiation of solubility. Decrease in pH value with increase in time is mainly because of an increase in solubility of glasses and decrease in sodium ions contents in glasses. Higher values of pH of SBF accelerate the formation of apatite as reported earlier by many researchers [42-44]. The variation in pH values ensures the exchange of ions between the glass and SBF solution. This may lead to form the apatite layer on the surface of the glasses.

4.2 Fourier Transform Infrared Spectroscopy

The infrared absorption spectra of the glasses under investigation have been recorded in order to obtain information about the possible changes of vibrational spectra due to the process of structural rearrangement with a change in glass composition. Figures 4.2 to 4.4 show the FT-IR of samples before and after the immersion in the simulated body fluid for 14 and 32 days.

Hydroxypatile $Ca_{10}(PO_4)_6(OH)_2$ has vibrational modes of phosphate and hydroxyls [45]. Table 4.1 shows the absorption IR bands for calcium phosphates.

Table 4.1: Characteristic calcium phosphate infrared absorption bands.

Absorption band	Wave number(cm^{-1})
OH^-	3572, 630
OH^- (H_2O)	3000-3700, 1600-1650
PO_4^{3-}	474, 562, 580, 640, 960-1200
P-OH	527, 870 , 910-1040

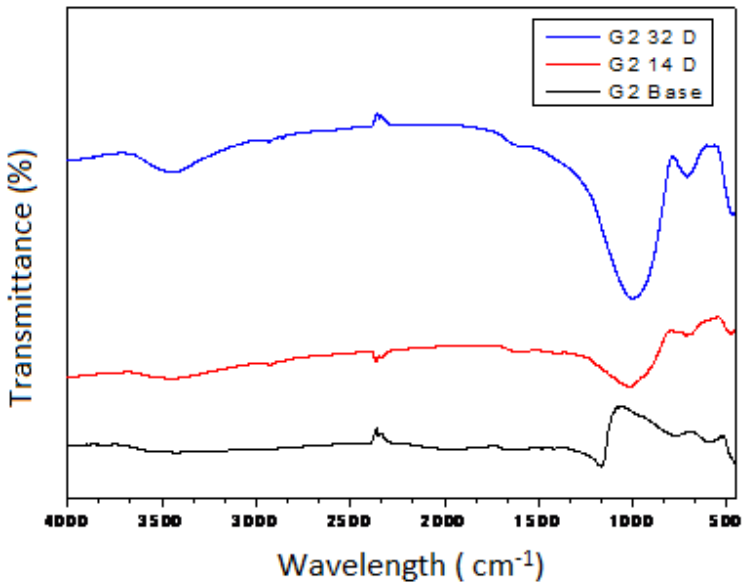

Figure 4.2: FTIR absorption spectra of sample G2 base, G2 14D,G2 31D, for virgin, 14 and 32 of soaking.

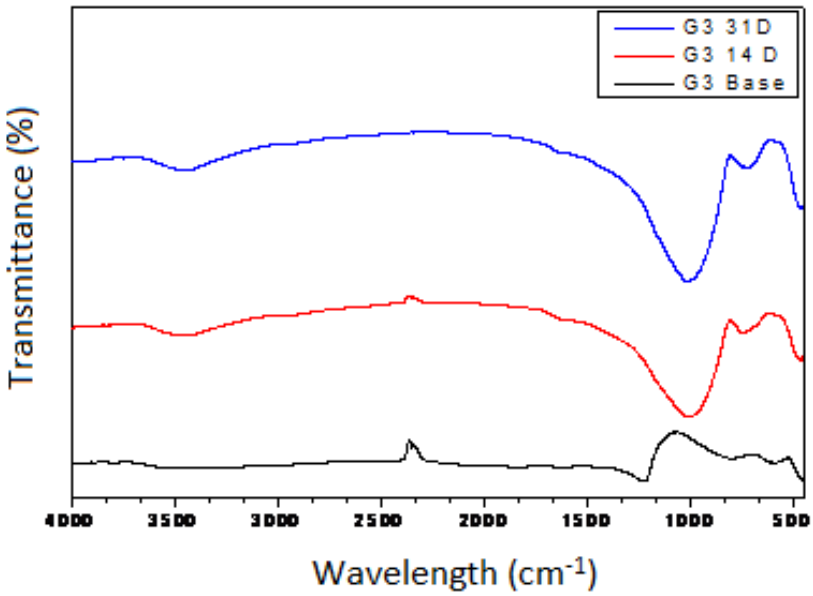

Figure 4.3: FTIR absorption spectra of sample G3 base, G3 14D, G3 31D, for virgin, 14 and 32 of soaking

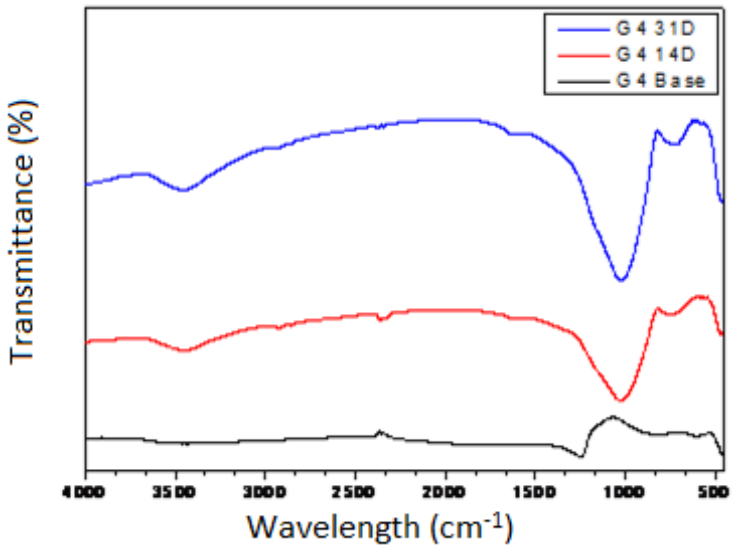

Figure 4.4: FTIR absorption spectra o0f sample G4 base, G4 14D, G4 31D, for virgin, 14 and 32 of soaking.

The spectrum of samples before immersion reveals the three main band of transmittance i.e. 400-510, 574-940 and 1110-1460 cm^{-1}. The band in the range from 400-650 cm^{-1} which is observed in all the glass samples is due to the Si-O-Si or O-Si-O bending modes. In the region from 574-940 cm^{-1} small kinks are also observed nearly about 568-650 cm^{-1} which can be due to $Si\text{-}O^{-}$ stretching with two non bridging oxygen and other kinks observed at 770-910 cm^{-1} which is due to the Si-O-Si symmetric stretching of bridging oxygen between tetrahedral coordination [35, 42].

The spectra of all soaked samples (14 and 32 days) shows a sharp bands at 480 cm^{-1},719 cm^{-1}, 1020 $cm^{-1}$and broad band at 3450 cm^{-1}. The broad absorption band at 3446 cm^{-1} is attributed to the stretching vibration of the OH group. The small absorption bands at 2924 cm^{-1}, 2848 cm^{-1}, 1589 cm^{-1} are attributed to the stretching vibration of the H-O-H group [46]. The absorption band at 2360 cm^{-1} is attributed to the presence of CO_2 in the measuring chamber of the device in which the specimen was placed, and is part of the equipment's background noise [47-48]. The absorption band at 720 cm^{-1} and 1380 cm^{-1} attributed to CO_3^{2-} , the absorption sharp band at 585 cm^{-1}, 585 cm^{-1} and 729 cm^{-1} are attributed due to P-HO stretching. The absorption sharp band at 480 $cm^{-1}$and 1020 cm^{-1} are attributed to PO_4 group. While bands close to 480 cm^{-1} are related to P-O deformation

vibrations of PO_4^{3-} group. A sharp P-O bending mode doublet at 478 cm^{-1} confirmed the presence of HA layer, which have been deposited on surface of glass samples. These finding are also supported by pH and EDX measurement.

4.3 XRD analysis

The XRD spectra for all the as prepared glasses G 2, G 3 and G 4 exhibit the characteristic amorphous hump. A typical X-ray diffraction pattern of G 2 , G 3, G4 samples before and after dipping in SBF solution, is given in figures 4.5 to 4.16,

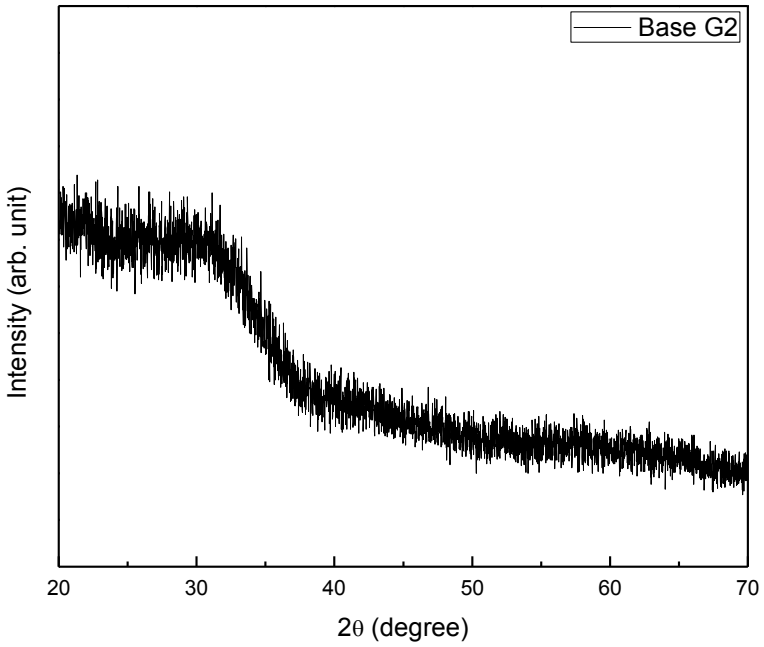

Figure 4.5: XRD pattern of G2 base glass.

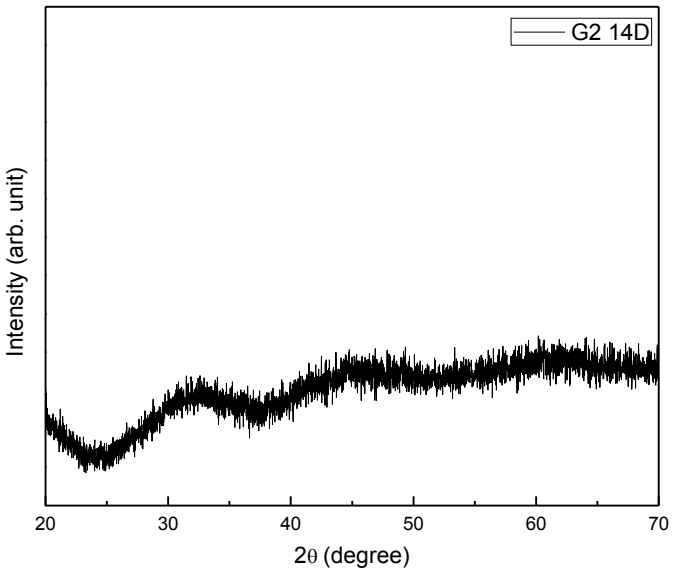

Figure 4.6: XRD pattern of sample G2 14D after dipping in SBF solution for 14 days.

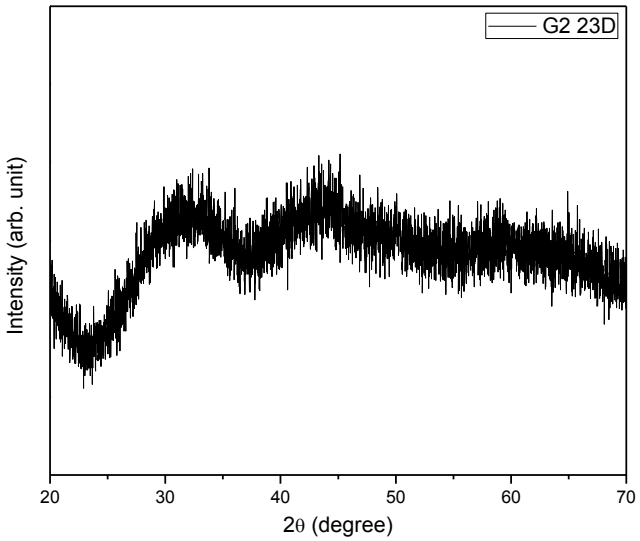

Figure 4.7: XRD pattern of sample G2 23D after dipping in SBF solution for 23 days.

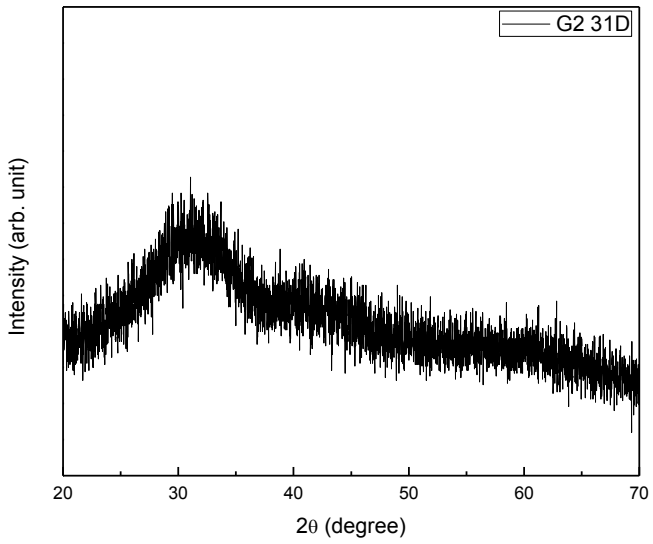

Figure 4.8: XRD pattern of sample G2 31D after dipping in SBF solution for 32 days.

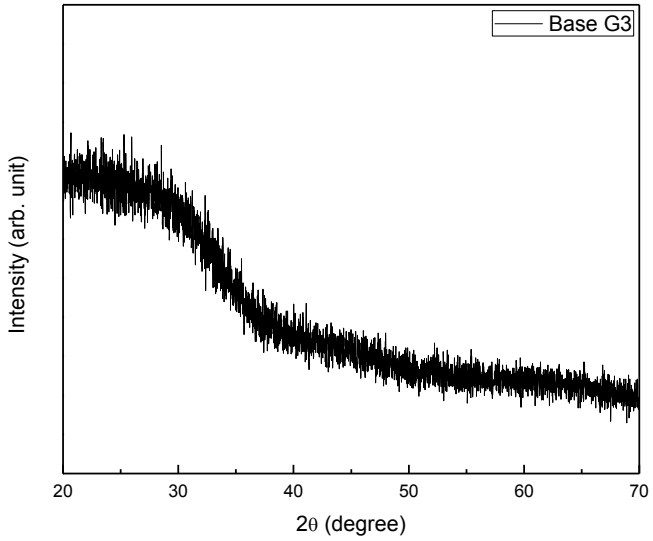

Figure 4.9: XRD pattern of sample G3 base.

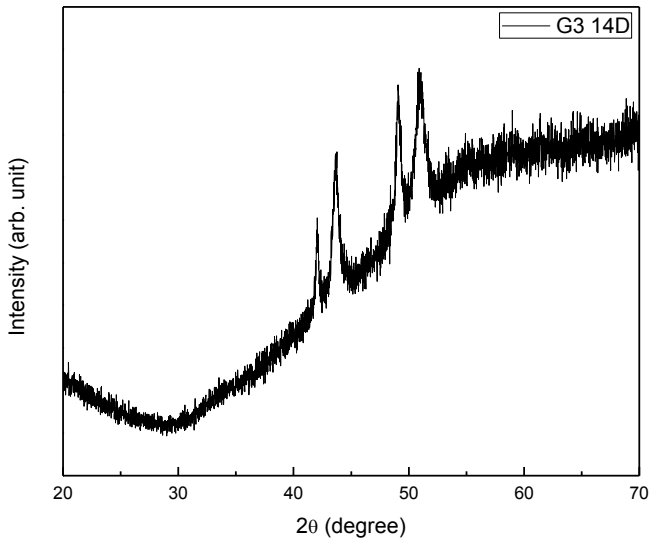

Figure 4.10: XRD pattern of sample G3 14D after dipping in SBF solution for 14 days

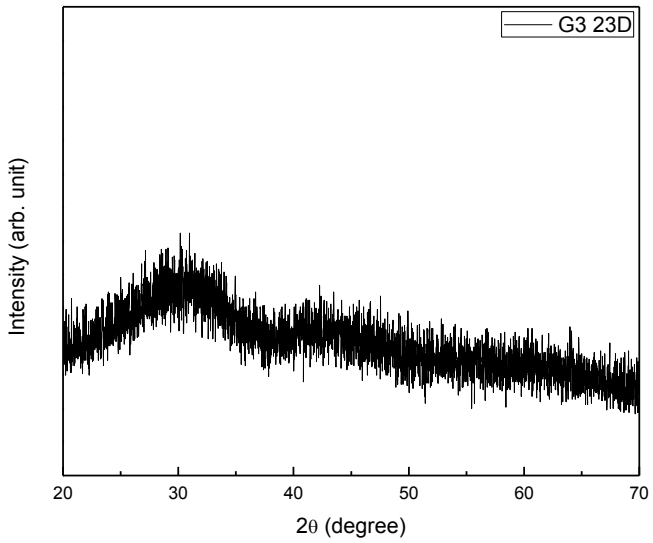

Figure 4.11: XRD pattern of sample G 3 23D after dipping in SBF solution for 23 days.

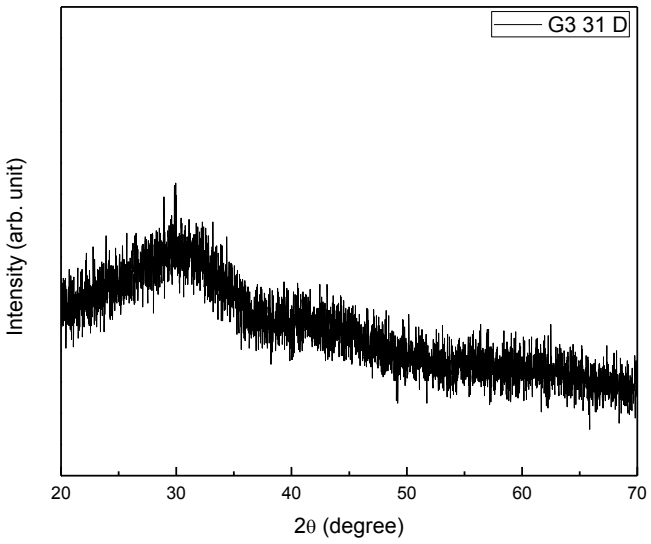

Figure 4.12: XRD pattern of sample G3 31D after dipping in SBF solution for 31 days.

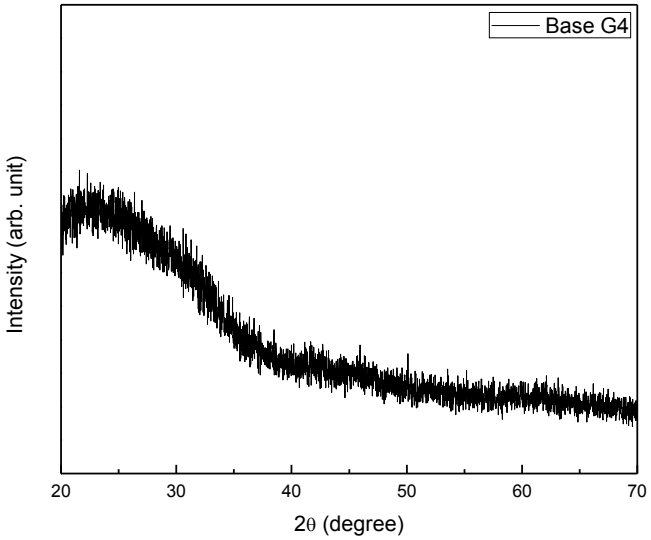

Figure 4.13: XRD pattern of sample G4 base glass.

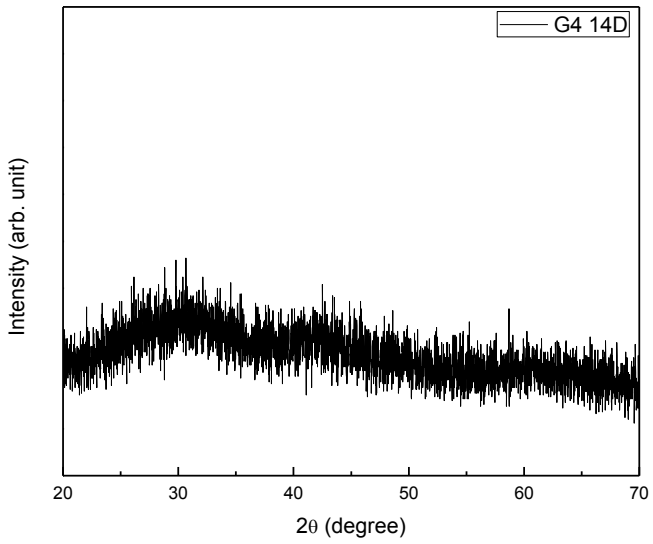

Figure 4.14: XRD pattern of sample G4 14D after dipping in SBF solution for 14 days.

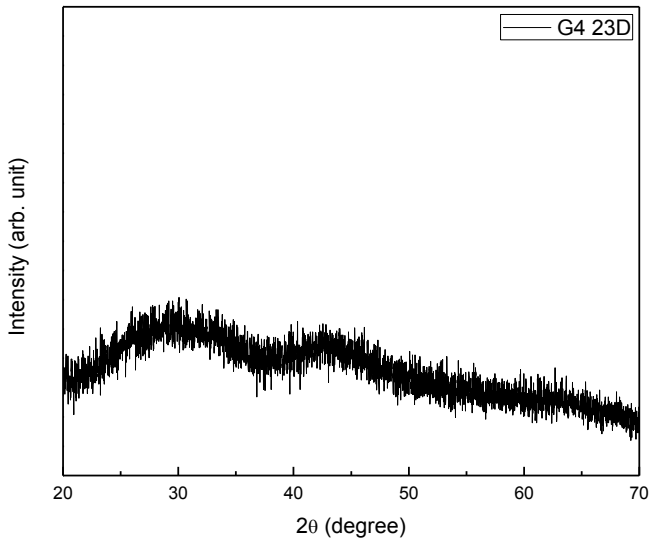

Figure 4.15: XRD pattern of sample G4 23D after dipping in SBF solution for 23 days.

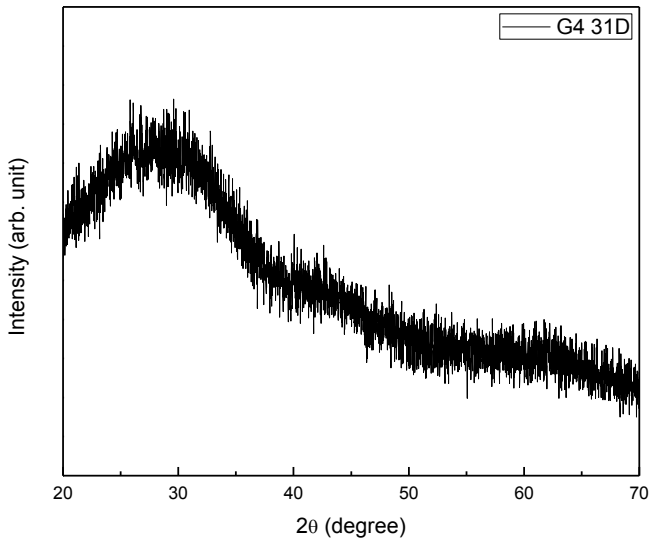

Figure 4.16: XRD pattern of sample G4 31D after dipping in SBF solution for 31 days.

The XRD pattern of all glasses shows some changes and modification in hump after dipping in SBF solution. This change can be attributed due to the formation of HA layer after dipping in the SBF solutions. These changes are prominent as the Na_2O content increases with respect to the glass network former (SiO_2) crystalline peaks are absent as reported in our earlier work Indu et al. [49] Obviously, the network modifier loose the glass network and reduce the covalency characteristics in network which may lead to higher dissolution of ions in SBF Solution

4.4 Energy band gap measurement

The band gap of before and after dipping samples are measured using UV-Visible Spectroscopy. These results give further insight of the hydroxyapatite layer formation after dipping in SBF solution. In other words, if a layer is forming on the surface of the sample, after dipping, due to the reaction between SBF solution and glass samples, then the band gap must hν versus $(\alpha h\nu)^2$. Based on these calculations the band gap of the soaked and unsoaked are estimated with decreasing content of Na_2O. It is well reported in the literature that the introduction of the modifier in glass composition may change the

optical band gap of the samples. The values of optical band gap decreases with the increase of Na_2O on the cost of SiO_2 in glasses composition. This can be explained on the basis of bonding defects and non bridging oxygen (NBO) which creates due to addition of Na_2O in glasses composition. It may lead to an increase of the degree of localization of electron there by the increase of donor center in glasses. Saritha et al [50] have reported that the introduction of heavy metal oxide (Bi_2O_3) in glass decrease the optical band gap. The change in optical band gap is attributed to the structural changes due to the different side occupancies by cations. Interestingly after soaking glasses in SBF solution, all glasses show the decreasing trend in optical band gap. Which may be possible due to some content leached out from the glasses during soaking. However, the band gaps of the soaked glasses could not show any trend with respect to the dipping duration. It indicates that the formation of apatite layer in early stage of the dipping. However in longer duration of dipping, the formation of apatite layer might be dissolved

Table 4.2: Soaking time and optical band gap of different glass samples.

Sample Name	Soaking time (hours)	Optical band gap
Base G2	0	5.2
G2 14D	52	4.0
G2 31D	750	5.1
BaseG3	0	4.8
G3 14D	52	3.96
G3 31D	750	4.65
Base G4	0	4.6
G4 23D	52	3.41
G4 31D	750	4.01

The higher presence of donor center leads to the decrease of optical band as observed in the present glasses.

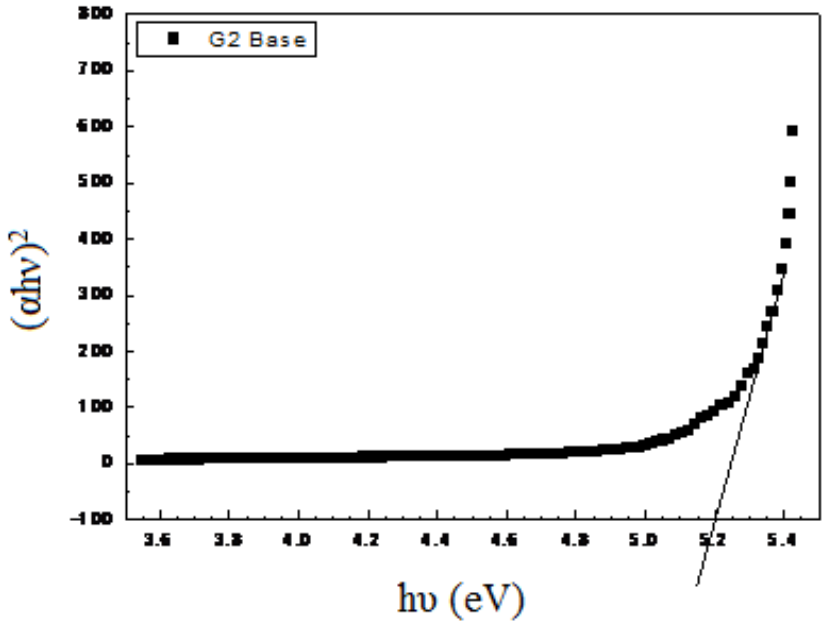

Fig 4.17: Band gap curve of G 2 base glass before dipping in SBF solution.

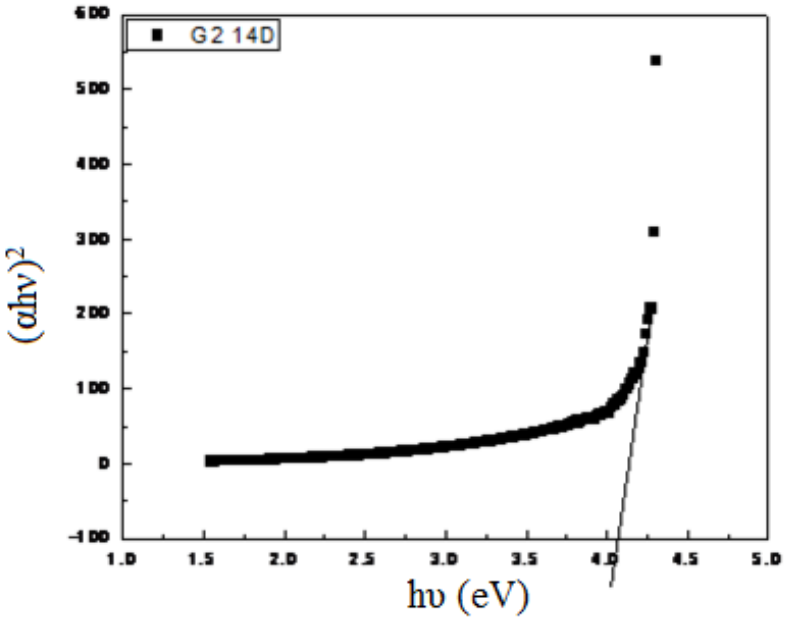

Fig 4.18: Band gap curve of G2 14D after dipping in SBF solution for 14 days.

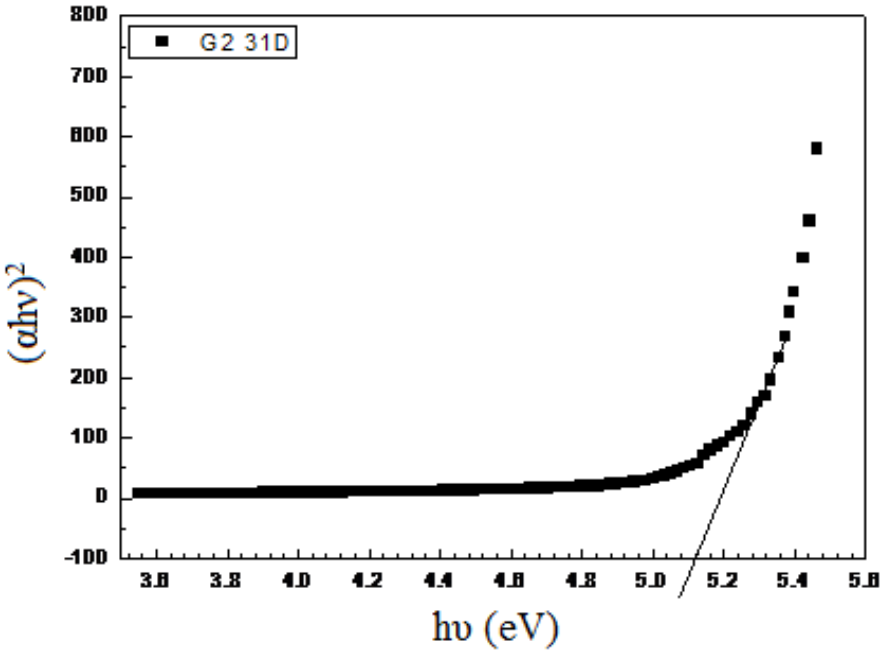

Fig 4.19: Band gap curve of G2 31D after dipping in SBF solution for 31 days.

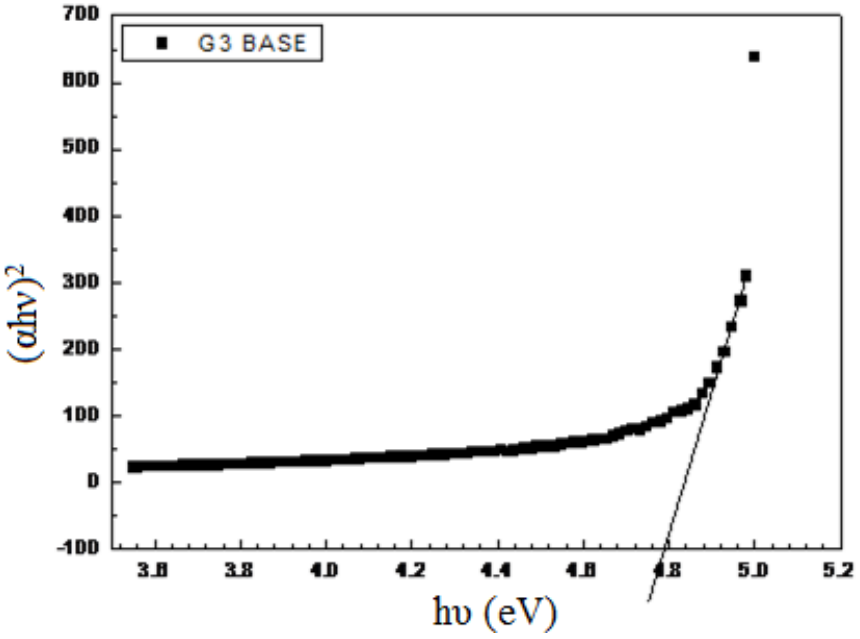

Fig 4.20: Band gap curve of G 3 base glass before dipping in SBF solution.

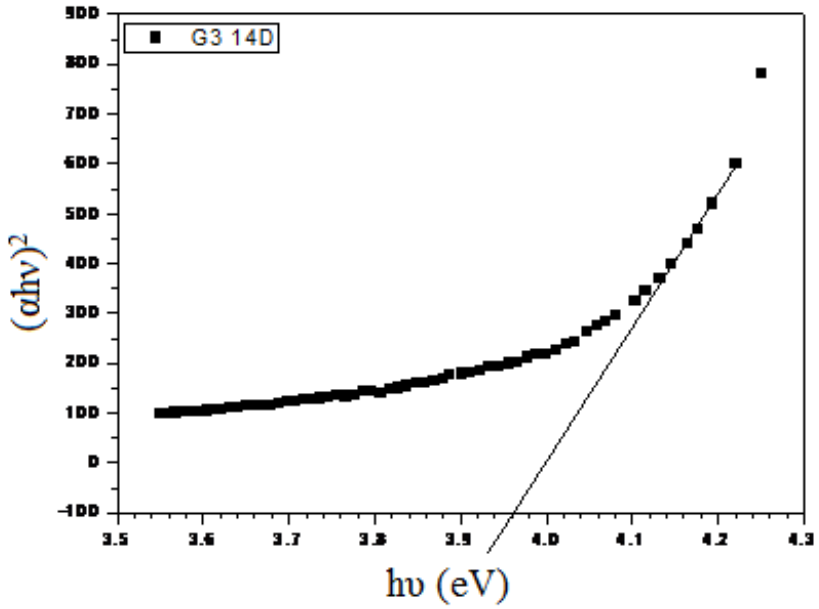

Fig 4.21: Band gap curve of G3 14D after dipping in SBF solution for 14 days.

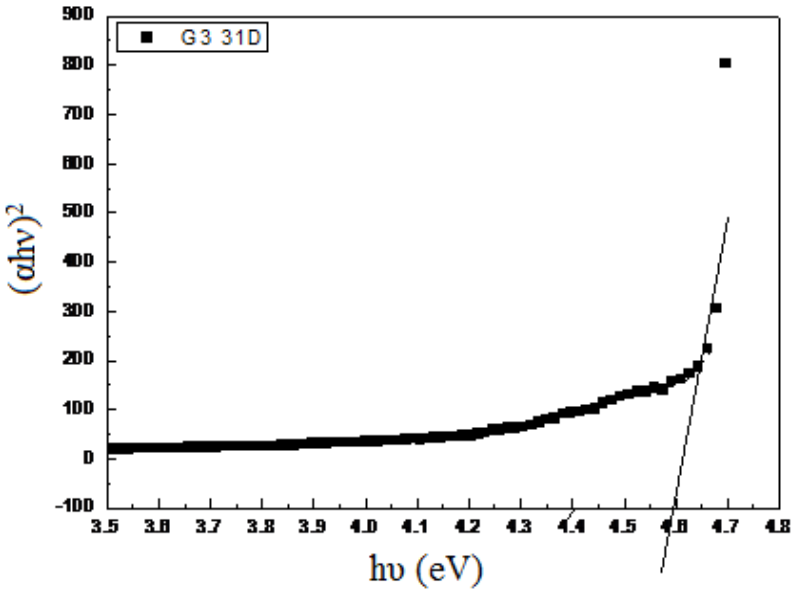

Fig 4.22: Band gap curve of G3 31D after dipping in SBF solution for 14 days.

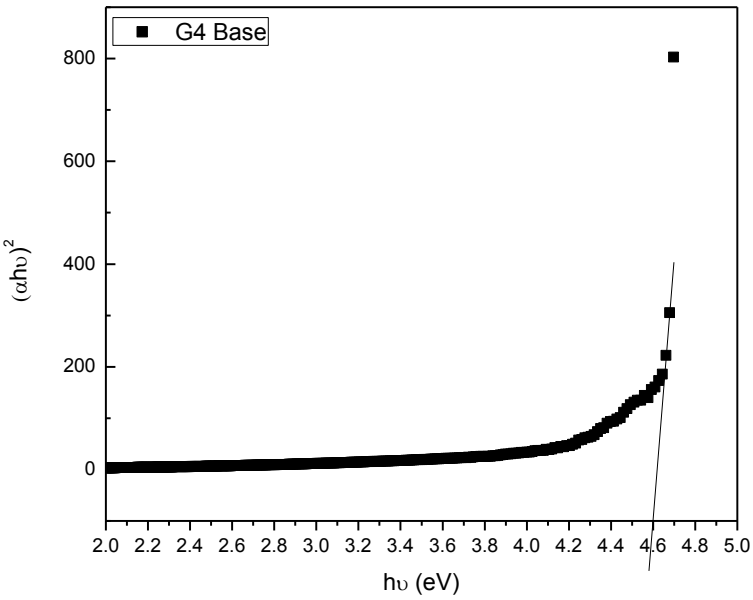

Fig 4.23: Band gap curve of G 4 base glass before dipping in SBF solution.

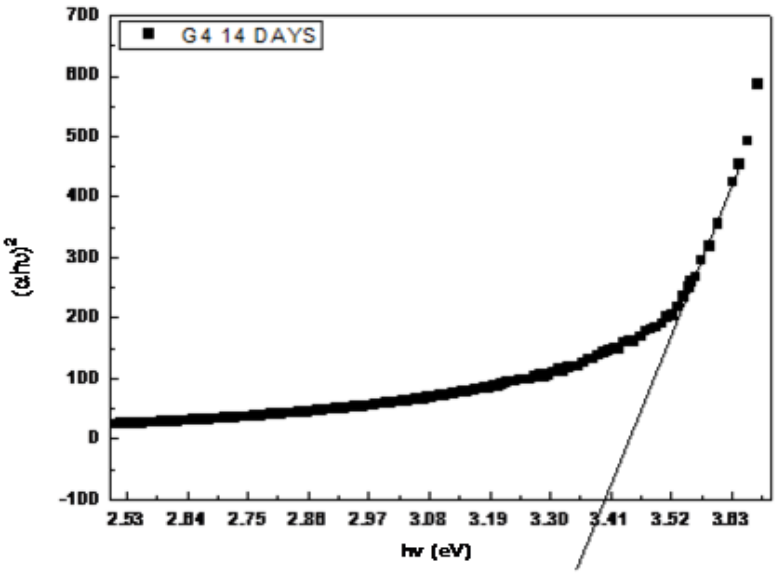

Fig 4.24: Band gap curve of G4 14D after dipping in SBF solution for 14 days.

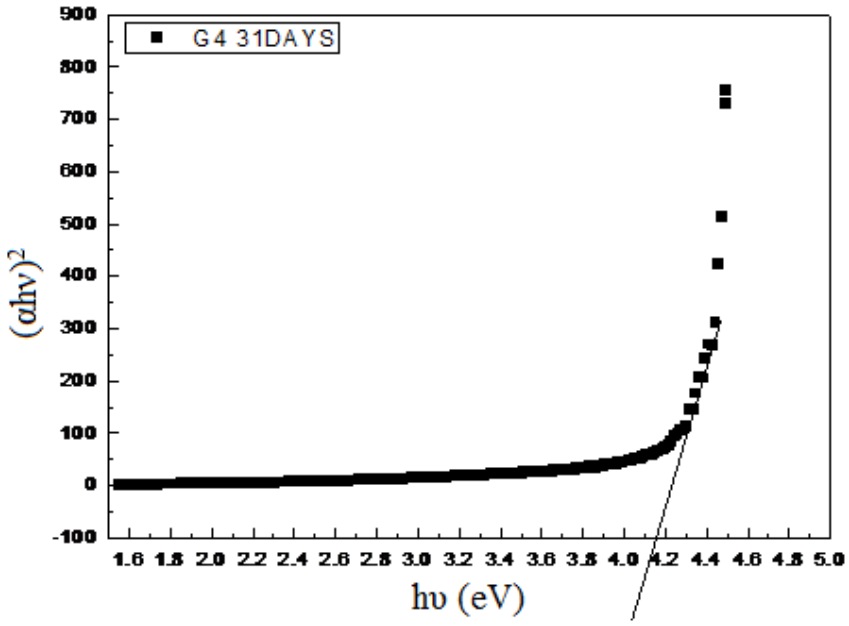

Fig 4.25: Band gap curve of G4 31D after dipping in SBF solution for 31 days.

4.5 Scanning electron microscopy (SEM)

The SEM and EDX analysis was done on the selected samples. The SEM micrograph of soaked samples show some changes on the surface of the glasses. All SEM micrographs were taken at the same magnification for comparing the results. The SEM micrograph of G2, G3, G4 samples after dipping for 23 days were shown in figs 4.26 to 4.29, respectively. The surface of the glasses exhibit equal particle distribution. The particle are more or less circular in shape. The distributions of the particles are more uniform in G2 glasses as compare to the other glasses. G1 glass has lower content of modification (Na_2-O). The FTIR, XRD and band gap measurement of these glasses show that the higher content of SiO_2, (G4) exhibit higher tendencies to form the hydroxyapatite layer as indicated by given SEM micrographs.

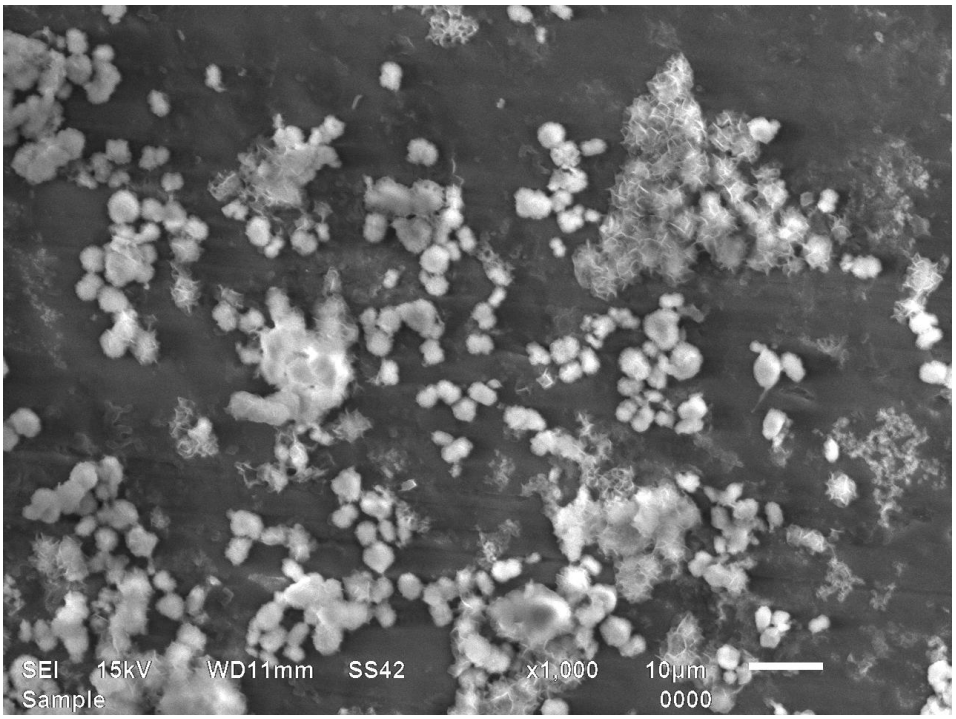

Fig 4.26: SEM of sample G2 14D after dipping in SBF solution for 23 days.

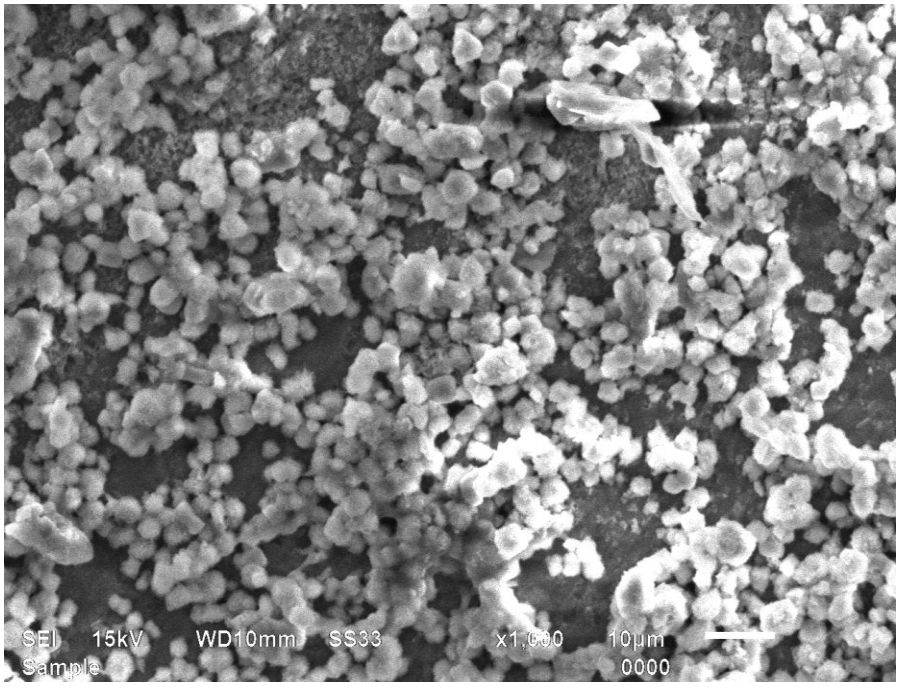

Fig 4.27: SEM of sample G2 23D after dipping in SBF solution for 23 days.

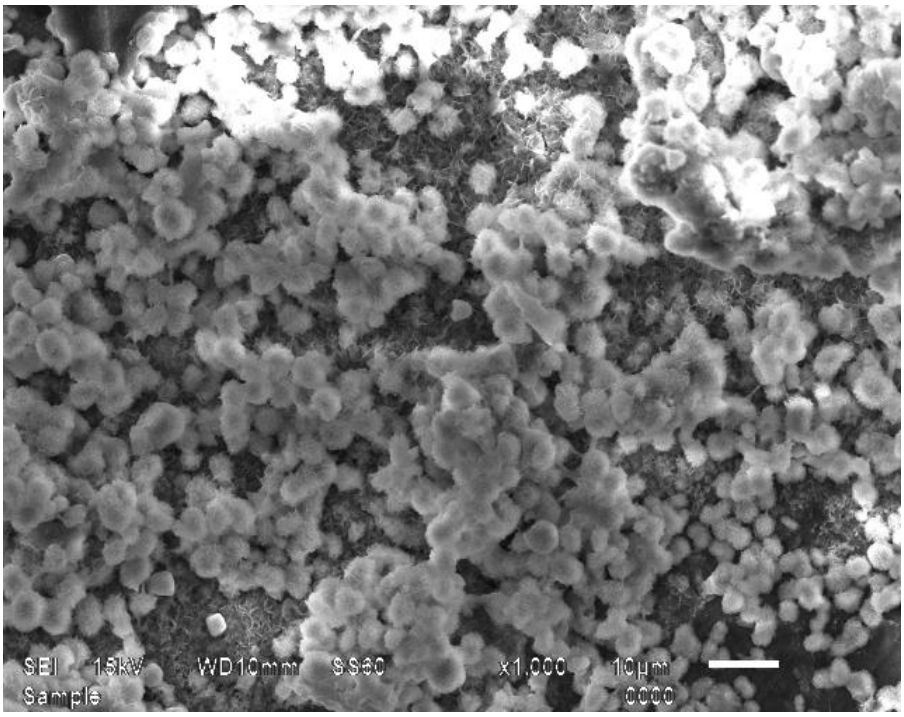

Fig 4.28: SEM of sample G3 23D after dipping in SBF solution for 23 days.

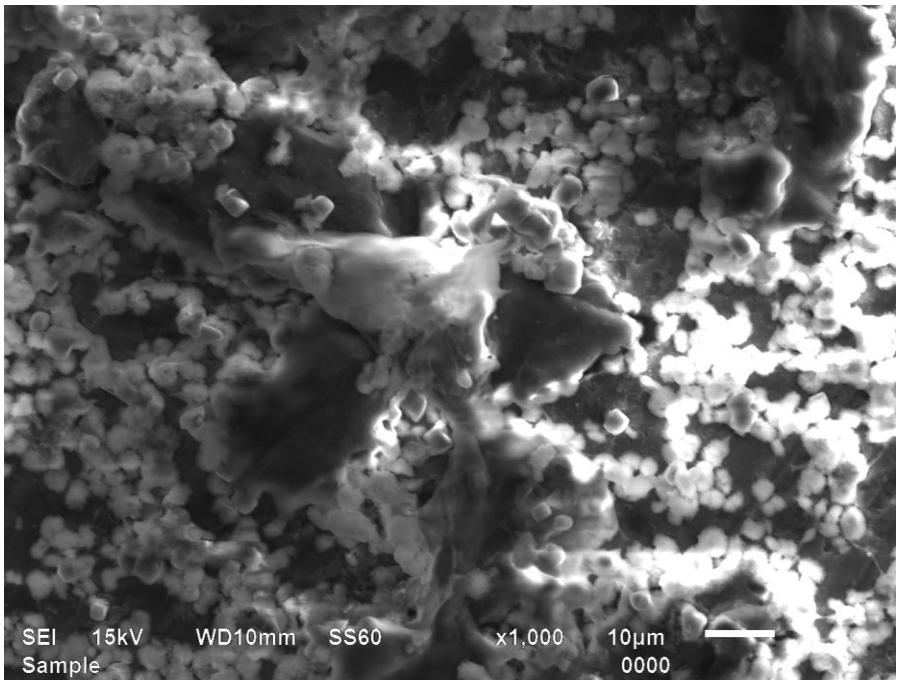

Fig 4.29: SEM of Sample G4 23D after dipping in SBF solution for 23 days.

4.6 Energy Dispersive Spectrometer (EDS)

The formation of the hydroxyapatite layer was further confirmed by the EDS analysis. The EDS analysis was done on the G3 sample after dipping 23 days in SBF solution. EDX analysis clearly indicates the presence of phosphate ions as shown in the table 4.3 and 4.3 to 4.4 along with micrograph. Fine granular deposits have been observed in all the glasses. Similar observations have been reported by Shunsuke Fujibayashia et al. [51].The white spot in micrographs show the higher presence of P^{+}, O^{2-} and Ca^{2+} which may be related to the hydooxyapatite layer on the glass[52-53]. However, the point analysis exhibits different concentration of element at the different places as shown in fig 4.30 to 4.31

Fig 4.30: EDX of Sample G4 23D after dipping in SBF solution for 23 days

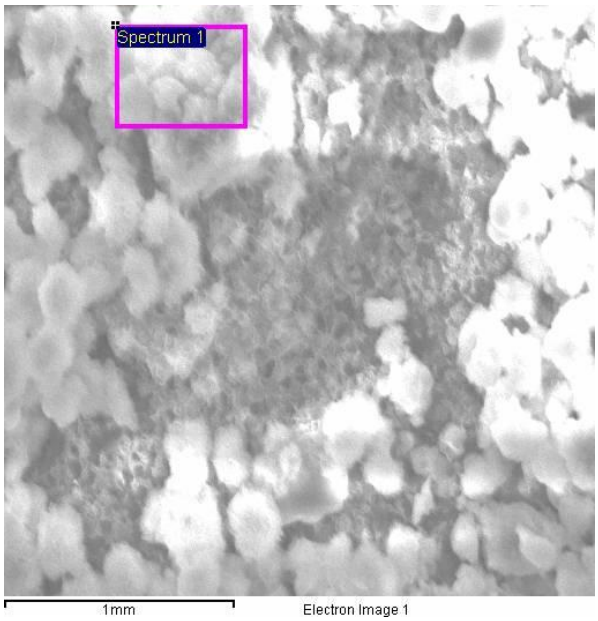

Table 4.3: Composition of elements in white layer of G4 23D by EDS

Element	Weight %	Atomic%
C K	24.97	35.12
O K	48.22	50.19
Na K	3.86	2.84
Mg K	0.62	0.43
Si K	0.20	0.12
P K	8.29	4.52
Cl K	4.20	2.00
K K	0.23	0.10
Ca K	9.40	3.96
Total	100	

Fig 4.31: EDX of Sample G4 23D after dipping in SBF solution for 23 days

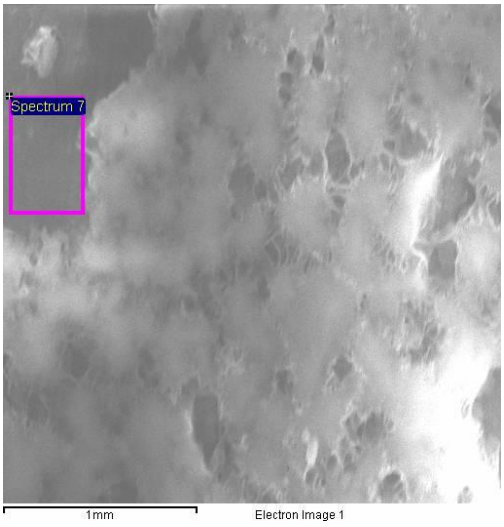

Table 4.4: Composition of elements in black portion of G4 23D by EDS

Element	Weight %	Atomic%
C K	5.8	8.94
O K	48.02	58.88
Na K	10.96	9.35
Mg K	6.98	5.07
Si K	18.23	12.74
P K	0.81	0.52
Cl K	0.72	0.40
K K	6.27	3.07
Ca K	2.54	1.04
Total	100	

In all glasses we compared and we concluded that granular shape is HA layer formation. It was formed in 1-2 weeks and dissolved in later weeks.

CHAPTER-5

CONCLUSIONS AND FUTURE SCOPE REFERENCES

In present investigation, three glass samples were selected with variable mol % Na_2O to check their bioactivity. These samples were characterized using XRD, SEM, EDX, FT-IR, UV-Vis spectroscopy and pH measurement. The durability of samples was checked in SBF solution in the form of weight loss and change in pH valves after soaking 31 days in SBF solution. However the change in pH, weight loss measurement, and XRD pattern shows some changes in the glasses after dipping in SBF solution which indicates the amorphous layer might be formed on the surface of the samples. Higher presence of modifier reduces the durability of the glasses. Higher modifier content decrease the optical after soaking the band gap decrease due to creation of donor center in glass matrix. The modification in XRD and presence of hydoxyle group in FTIR indicate the formation of amorphous hydroxyapatite layer. The EDS and SEM measurement is further confirmed the formation of apatite layer.

Future Scopes

As indicated by the results of the present study, the soaking time might be increased to study the effect on the formation of crystalline apatite layer. Higher content of Na_2O in initial ingredients of glass can be investigated to study the effect on dissolution, durability of glasses in SBF solution.

REFERENCES

1. J.B. Brunski. Metals, Biomaterials Science: An Introduction to Materials in Medicine 37-50, Academic Press, San Diego (1996)
2. L.L. Hench. Ceramics, Glasses, and Glass-Ceramics, 73–84
3. J.B. Park and R.S. Lakes, Biomaterials, Plenum Press, New York (1992)
4. J. Black, Biological Performance of Materials, Marcel Dekker, New York (1992)
5. J. Kohn and R. Langer. Bioresorbable and Bioerodible Materials, 64–73
6. J.B. Park and R.S. Lakes, Biomaterials, Plenum Press, New York (1992)
7. P.K. Kundu, T.S. Waghode, D. Bahadur, D. Datta, Med. Biol. Eng. Computer, 36, 654–658 (1998)
8. U.O. Hafeli, G. J. Pauer, J. Magn. Magn. Mater. 194, 76–82 (1999)
9. S Golui, D Datta, D Bahadur , Proc. 8th Int. Conf. on ferrites (ICF 8) Kyoto, Japan, 105 (2000)
10. Laurel Sheppard,"How bioceramics are made?" 67 July (1998)
11. L L Hench and June Wilson,"Introduction to bioceramics". World Scientific,Singapore (1993)
12. T. Ebisawa ,T.kokubo,K. Ohura,T. yamamura,"Fatigue and Lifetime of bioactive glass ceramics containing apatite and wollastanite", J.Mater , Sci 22 4067 (1987)
13. L L Hench, R J Spinter, W C Allen, T K Greenlee, Bonding mechanism at the interface of ceramic prosthetic materials, J. Biomed Mater.Res.2, 117 (1971)
14. L L Hench, H A Paschall, Direct chemical bond between bioactive glassceramic material and bone, J. Biomed Mat. Res. Symp. 4, 25 (1973)

15. L. L Hench. Anderson O Bioactive glasses. L L Hench, Wilson J (Eds.), An introduction to Bioceramics. World Scientific, Singapore. (1993)

16. A. Nishara Begum, V. Rajendran, Materials Chemistry and Physics 96,409 (2006)

17. W Vogel, W Holan, Development, structure, properties and applications of glassceramics for medicine, J. Non-Cryst. Solids, 1223 (1990)

18. T Kokubo, S Ito, S Sakka, T Yamamuro, J. Mater, Sci. 21, 536 (1986)

19. K. El-Egili, Physica B 325,340 (2003)

20. K. Franks, I. Abrahams, J. C. Knowles, Development of soluble glasses for biomedical use Part I: In vitro solubility measurement, Journal of Materials Science: Materials in Medicine 11, 609-614 (2000)

21. T Kokubo, Surface Chemistry of Bioactive Glass-Ceramics, J. Non-Cryst. Solids, 120, 138 (1990)

22. Sahil Jalota, Sarit B. Bhaduri, A. Cuneyt Tas, Using a synthetic body fluid (SBF) solution of 27 mM HCO_3^- to make bone substitutes more osteointegrative, Materials Science and Engineering C 28, 129–140 (2008)

23. J.M. Oliveira, R.N. Correia and M.H. Fernandes, Biomaterials 16,649 (1995)

24. V.Simon, C, Albonand, S. Simon, Journal of non-crystalline solids, in press, corrected proof cot (2007)

25. A. Rapacz-Kmita, C. Paluszkiewicz ,A. SI ,loIsarczyka ,Z.Paszkiewicza, Journal of Molecular Structure 744 (2005)

26. Y Kim, S S Jee, Hydroxyapatite formation on bioactive-glazed alumina, J. Europ. Ceram. Soc., 23, 1803 (2003)

27. Y Ebisawa, T Kokubo, K Ohura, T Yamamuro, Bioactivity of CaO.SiO2-based glasses: In vitro evaluation, J.Mater Sci. Mater. Med. 1,239 (1990)

28. J Roman, A J. Salinas , M Vallet-Regi, J M Oliveira, R N Correia, M H Fernandes, Role of acid attack in the vitro bioactivity of a glass-ceramic of the 3 CaO. P2O5-CaO.SiO2-CaO. MgO.2SiO2 system. Biomaterials, 22, 2013 (2001)

29. J.A. Sanz-Herrera, A.R. Boccaccini. Modelling bioactivity and degradation of bioactive glass based tissue engineering scaffolds. International Journal of Solids and Structures, 48, 257–268 (2011)

30. B. Saravanakumar, M. Rajkumar, V. Rajendran, Synthesis and characterisation of nanobioactive glass for biomedical applications. Materials Letters, 65,31–34 (2011)

31. O.M. Goudouria, E. Kontonasakib, A. Theocharidoub, L. Papadopoulouc, N. Kantiranisc, X. Chatzistavroua, P. Koidisb, K.M. Paraskevopoulosa, Materials Chemistry and Physics, 125, 309–313 (2011)

32. V. Cannillo, J. Colmenares-Angulo, L. Lusvarghi, F. Pierli, S. Sampath, "In vitro characterisation of plasma-sprayed apatite/wollastonite glass–ceramic biocoatings on titanium alloys", Journal of the European Ceramic Society, 29, 1665–1677 (2009)

33. Anu Arora ," Studies on SiO2-BaO-ZnO-(M2O3)x-(B2O3)1-x(M= Al, Mn, Y, La) Based glasses sealents" (2009)

34. O Peitl, G P L Torre, L L Hench, Effect of crystallization on apatite-layer formation of bioactive glass 45S5, J. Biomed. Mater. Res. 30, 509 (1996)

35. Qi-Zhi Chen, Yuan Li, Li-Yu Jin, Julian M.W. Quinn, Paul A. Komesaroff, A new sol–gel process for producing Na2O-containing bioactive glass ceramics, Acta Biomaterialia 6, 4143–4153 (2010)

36. G.Y. Liu, J. Hu, Z.K. Ding, C. Wang, Bioactive calcium phosphate coating formed on micro-arc oxidized magnesium by chemical deposition, Applied surface Science 257, 2051- 2057 (2011)

37. Mineo Hashizumea,∗, Yuka Nagasawaa, Tomohiko Suzukia, Shin awashimaa,Masanobu Kamitakaharab, Effect of preparative conditions on crystallinity of apatite particles obtained fromsimulated body fluids, Colloids and Surfaces B: Biointerfaces 84, 545–549, (2011)

38. J.P. Nayak, S. Kumar, J. Bera , Sol–gel synthesis of bioglass-ceramics using rice husk ash as a source for silica and its characterization, Journal of Non-Crystalline Solids 356, 1447–1451 (2010)

39. L.L. Hench, CRC Handbook of bioactive glasses and glass ceramics.CRC Press, Boca Raton, FL (1990)

40. Wu Tie, He Ouli, Xiu Zengzou, Gong Fangtian and Zhou Ao, Effect of Al_2O_3 on phase separation and crystallization in ZnO-$Al_2O.B_2O_3$-SiO_2 glasses, Research Institute of Building Materials, Beijing, PRC (2003)

41. Changsheng Liu, Yue Huang, Wei Shen and Jinghua Cui**,** People's Republic of China,130 (2000)

42. A. Cuneyt Tas, Synthesis of biomimetic Ca-hydroxyapatite powders at 373^{o}C in synthetic body fluids, Biomaterials, 21, 1429-1438 (2000)

43. EC Moreno, K Varughese, Crystal growth of calcium apatites from dilute solutions, J Crystal Growth, 53, 20-30 (1981)

44. JC Haugbert, SJ Zawacki, GH Nancollas. The growth of octacalcium phosphate on b tricalcium phosphate, J Crystal Growth, 90,63-83 (1983)

45. Frank A. Mullera, Lenka Mullera, Daniel Caillard, Egle Conforto, Preferred growth orientation of biomimetic apatite crystals, Journal of Crystal Growth, 304, 464–471 (2007)

46. C. Paluszkiewicz , M. Blaz˙ ewicz, J. Podporska, T. Gumuła, Nucleation of hydroxyapatite layer on wollastonite material surface: FTIR studies, Vibrational Spectroscopy, 48, 263–268 (2008)

47. K. Franks, I. Abrahamsi, J. C. Knowles ,Development of soluble glasses for biomedical use Part I: In vitro solubility measurement , Journal of materials science: Materials in medicines 11, 609-614 (2000)

48. C. Berbecarua, H.V. Alexandru, G.E. Stan, D.A. Marcov, I. Pasuk, A. Ianculescu, First stages of bioactivity of glass-ceramics thin films prepared by magnetron sputtering technique, Materials Science and Engineering B, 169, 101–105 (2010)

49. Indu Bala, K. Singh, Vishal Kumar, Structural, optical and bioactive propertites of calcium of calcium borosilicate glasses, Ceramics International,35, 3401-3406 (2009)

50. D. Saritha, Y. Markandeya, M. Salagram, M. Vithal, A.K. Singh, G. Bhikshamaiah, J. Non- Crystal Solid 354, 5573 (2008)

51. Shunsuke Fujibayashia, Masashi Neoa, Hyun-Min Kimb, Tadashi Kokubob, Takashi Nakamura, A comparative study between in vivo bone ingrowth and in vitro apatite formation on Na2O–CaO–SiO2 glasses, Biomaterials, 24, 1349–1356 (2003)

52. C.R. Mariappan, D.M. Yunos, A.R. Boccaccini, B. Roling, Bioactivity of electro-thermally poled bioactive silicate glass, Acta Biomaterialia, 5, 1274–1283 (2009)

53. C.P. Yoganand, V. Selvarajan, Valeria Cannillo, Antonella Sola, E. Roumeli, O.M. Goudouri, K.M. Paraskevopoulos, Mahmoud Rouabhia, Characterization and in vitro-bioactivity of natural hydroxyapatite based bio-glass–ceramics synthesized by thermal plasma processing, Ceramics International 36, 1757–1766 (2010)